ผลของดินเหนียวดัดแปลงต่อสมบัติเชิงกล
และเชิงความร้อนของแผ่นเยื่อเซลล์เชื้อเพลิง

นาย พิชญ์ ศักดิ์วงศ์

วิทยานิพนธ์นี้เป็นส่วนหนึ่งของการศึกษาตามหลักสูตรปริญญาวิศวกรรมศาสตรมหาบัณฑิต
สาขาวิชาวิศวกรรมเคมี ภาควิชาวิศวกรรมเคมี
คณะวิศวกรรมศาสตร์ จุฬาลงกรณ์มหาวิทยาลัย
ปีการศึกษา 2551

EFFECTS OF MODIFIED ORGANO-CLAY ON THE MECHANICAL

AND THERMAL PROPERTIES OF FUEL CELL MEMBRANE

Mr. Pitch Sakwong

A Thesis Submitted in Partial Fulfillment of the Requirements

for the Degree of Master of Engineering Program in Chemical Engineering

Department of Chemical Engineering

Faculty of Engineering

Chulalongkorn University

Academic Year 2008

Thesis Title	EFFECTS OF MODIFIED ORGANO-CLAY ON THE MECHANICAL AND THERMAL PROPERTIES OF FUEL CELL MEMBRANE
By	Mr. Pitch Sakwong
Field of Study	Chemical Engineering
Advisor	Varun Taepaisitphongse, Ph.D.

Accepted by the Faculty of Engineering, Chulalongkorn University in Partial Fulfillment of the Requirements for the Master's Degree

.... Dean of the Faculty of Engineering

(Associate Professor Boonsom Lerdhirunwong, Dr.Ing.)

THESIS COMMITTEE

.... Chairman

(Associate Professor Paisan Kittisupakorn, Ph.D.)

.... Advisor

(Varun Taepaisitphongse, Ph.D.)

.... Examiner

(Professor Suttichai Assabumrungrat, Ph.D.)

.... External Examiner

(Associate Professor Somsak Woramongconchai, D.Eng.)

พิชญ์ ศักดิ์วงศ์ : ผลของดินเหนียวดัดแปลงต่อสมบัติเชิงกล และเชิงความร้อนของแผ่น
เยื่อเซลล์เชื้อเพลิง. (EFFECTS OF MODIFIED ORGANO-CLAY ON THE
MECHANICAL AND THERMAL PROPERTIES OF FUEL CELL MEMBRANE) อ. ที่
ปรึกษาวิทยานิพนธ์หลัก: อ.ดร. วรัญ แต้ไพสิฐพงษ์, 78 หน้า.

งานวิจัยนี้มุ่งศึกษาผลของปริมาณดินเหนียวมอนโมริลโลไนท์ดัดแปลงที่มีต่อสมบัติ
เชิงกลและเชิงความร้อนของแผ่นเยื่อเซลล์เชื้อเพลิงระหว่างนาฟิออน/ดินเหนียวมอนโมริลโลไนท์
ดัดแปลงที่ถูกเตรียมด้วยวิธีการผสมสารละลาย นาฟิออน เปอร์ฟลูออริเนท เรซิน (ร้อยละ 5 โดย
น้ำหนักใน อะลิฟาติกแอลกอฮอล์และน้ำ) ด้วยมอนโมริลโลไนท์ดัดแปลง (Bentone SD®1) ที่
ปริมาณ 0, 3, 6, และ 10 ส่วนต่อร้อยส่วนของเรซิน โครงสร้างของแผ่นเยื่อคอมพอสิตถูกศึกษา
โดยวิธีการกระเจิงแสงของรังสีเอ็กซ์ (XRD) ส่วนประสิทธิภาพของแผ่นเยื่อคอมพอสิตถูกศึกษาใน
รูปของการซึมซับน้ำ ความสามารถในการแลกเปลี่ยนไอออน และสมบัติเชิงกลและเชิงความร้อน
ของแผ่นเยื่อคอมพอสิต

ผลการศึกษาโดยวิธีการกระเจิงแสงของรังสีเอ็กซ์พบว่าระยะห่างของชั้นของแผ่น
ดินเหนียวลดลงเมื่อผสมดินเหนียวดัดแปลงลงไปในแผ่นเยื่อนาฟิออน ซึ่งอาจกล่าวได้ว่าสายโซ่
ของนาฟิออนไม่ได้สอดแทรกเข้าไประหว่างชั้นของดินเหนียวดัดแปลง ดังนั้นแผ่นเยื่อคอมพอสิตที่
เตรียมได้จึงเป็นแบบคอมพอสิตทั่วไป การซึมซับน้ำของแผ่นเยื่อคอมพอสิตที่ผสมดินเหนียว
ดัดแปลงมีค่าเพิ่มขึ้นตามปริมาณดินเหนียวดัดแปลงที่เพิ่มขึ้น แต่ค่าความสามารถในการ
แลกเปลี่ยนไอออนของแผ่นเยื่อคอมพอสิตที่ผสมดินเหนียวดัดแปลงมีค่าลดลง ค่าอิลาสติกมอ
ดูลัส (Elastic Modulus) ของแผ่นเยื่อคอมพอสิตที่ผสมดินเหนียวดัดแปลงที่อิ่มน้ำมีค่าประมาณ
เท่ากับค่าอิลาสติกมอดูลัสของแผ่นเยื่อนาฟิออน แต่ค่ายืดตัวที่จุดขาด (Elongation at Break)
ของแผ่นเยื่อคอมพอสิตที่ผสมดินเหนียวดัดแปลงที่อิ่มน้ำมีค่าต่ำกว่า ดังนั้นการเติมดินเหนียว
ดัดแปลงลงไปในแผ่นเยื่อนาฟิออนสามารถช่วยลดการเสื่อมสมบัติเชิงกลของแผ่นเยื่อคอมพอสิต
ได้โดยการหักล้างผลกระทบของปริมาณการซึมซับน้ำที่เพิ่มขึ้นในแผ่นเยื่อคอมพอสิต

ภาควิชา วิศวกรรมเคมี ลายมือชื่อนิสิต
สาขาวิชา วิศวกรรมเคมี ลายมือชื่ออ.ที่ปรึกษาวิทยานิพนธ์หลัก
ปีการศึกษา 2551

4970471321   : MAJOR CHEMICAL ENGINEERING

KEYWORDS: NAFION[®] / PROTON EXCHANGE MEMBRANE / CLAY

PITCH SAKWONG : EFFECTS OF MODIFIED ORGANO-CLAY ON THE MECHANICAL AND THERMAL PROPERTIES OF FUEL CELL MEMBRANE. THESIS ADVISOR : VARUN TAEPAISITPHONGSE, Ph.D., 78 pp.
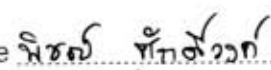
This work aimed to study the effects of modified Montmorillonite clay (m-MMT) loading on the mechanical and thermal properties of the Nafion[®]/m-MMT composite membrane prepared by solution mixing method. Nafion[®] perfluorinated resin (5 wt% in lower aliphatic alcohol and water) was mixed with m-MMT (Bentone SD[®]1) at 0, 3, 6, and 10 phr. The structures of the composite membranes were studied by XRD. Their performances were determined in terms of water uptake, ion exchange capacity (IEC), thermal and mechanical properties.

The XRD results showed that the interlayer spacing of m-MMT was decreased when incorporated into Nafion[®] matrix. Hence, the Nafion[®] matrix did not intercalate into interlayer spacing of m-MMT and the composite obtained was of a conventional composite type. The water uptake of Nafion[®]/m-MMT composite membrane increased with increasing amount of m-MMT in Nafion[®] matrix but the IEC values of Nafion[®]/m-MMT composite membranes decreased. These effects would balance each other out and the proton conductivity of Nafion[®]/m-MMT composite membranes would not differ from the pristine Nafion[®] membrane. The elastic moduli of soaked Nafion[®]/m-MMT composite membranes were about equal to the soaked pristine Nafion[®] membrane but the elongation at break of the soaked Nafion[®]/m-MMT composite membranes were lower. Therefore, the incorporation of this m-MMT into Nafion[®] matrix at least helped reduce the decay of these mechanical properties by counteracting the effects of increasing water uptake in the composite membranes.

Department : .....Chemical Engineering   Student's Signature ....

Field of Study : ...Chemical Engineering....   Advisor's Signature...........................

Academic Year : ....2008.........................

ACKNOWLEDGEMENTS

CONTENTS

LIST OF TABLES

LIST OF FIGURES

FIGURE   PAGE

ศูนย์วิทยทรัพยากร
จุฬาลงกรณ์มหาวิทยาลัย

CHAPTER I

INTRODUCTION

1.1 Introduction

At present, many countries in the world are concerning about global warming because an increase in global temperature can cause environmental changes and increase frequency and intensity of extreme weather events such as rising sea level, glacier retreat, hurricanes, heat waves, floods and droughts. Moreover, the other possible consequences are species extinctions, decreased agricultural yields and mutation of insects or microbes. The main cause of global warming is an increase of greenhouse gases such as carbon dioxide and methane in the atmosphere. The greenhouse gases are created by burning of fossil fuels from power stations, industrial processes, transportation and other human activities [1].

There are many ways to reduce greenhouse gases emission; fuel cell is one of many strategies [2]. Fuel cell is an electrochemical device that converts directly from chemical energy to electrical energy. Polymer electrolyte membrane fuel cell (PEMFC), one type of fuel cells, reacts hydrogen and oxygen to produce electricity and water without generating greenhouse gases [3]. Polymer electrolyte membrane fuel cell can be used for power generation in transportation.

The important part of PEMFC is electrolyte membrane which the most commercially available is Nafion® membrane [4]. Nafion® membrane is perfluorosulfonic acid (PFSA) polymer membrane. The molecular structure of PFSA membrane consists of Teflon-like backbone with sulfonic acid ($-SO_3H$) side chain. Nafion® membrane shows some excellent properties such as chemically inert, high proton conductivity and some disadvantages such as high methanol permeability [4]. In previous works [4, 5, 7-11], there were many attempts to reduce the methanol permeability and improve proton conductivity of Nafion® membrane by preparing Nafion®/Montmorillonite composite

membrane. Nafion[®]/Montmorillonite composite membranes have not only reduced methanol permeability, but still have the same conductivity of commercial membranes [4]. Two methods have been employed to prepare composite membranes: (1) direct addition of particles to a solution of Nafion[®], followed by casting; (2) impregnation of membranes with solutions of inorganic precursors and in situ sol-gel reaction to produce a metal oxide [12]. However, there are no reports on the modification of mechanical properties of Nafion[®]/Montmorillonite composite membrane. Therefore, this work studied the mechanical and thermal properties improvement of Nafion[®]/Montmorillonite composite membrane by solution mixing method.

1.2 Objective

This work aimed to study the effects of modified Montmorillonite clay (m-MMT) loading on the mechanical and thermal properties of the Nafion[®]/m-MMT composite membrane.

CHAPTER II

THEORY

2.1 Fuel Cell

Fuel cell is an electrochemical device that converts directly from chemical energy to electrical energy without burning or combustion of fuel. The schematic of fuel cell is shown in Figure 2.1. Fuel cell consists of an electrolyte between two electrodes. One electrode, called anode, produces protons and electrons from hydrogen by the oxidation reaction. Electrons pass through the external circuit, thus generating electricity, to another electrode, called cathode, and the reduction reaction occurred by electrons, protons and oxygen. The product of the reduction reaction is water. Therefore, the fuel cell does not generate pollution gases or greenhouse gases [13].
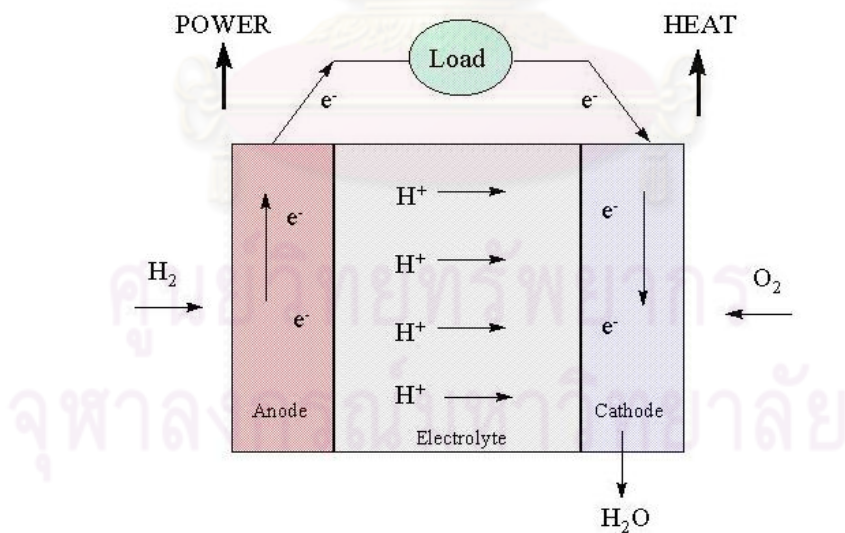
Figure 2.1 Schematic of Fuel Cell [14]

2.2 Types of Fuel Cells

Fuel cells are classified by their kind of electrolyte, reactant, catalyst, operating temperature range and others. The applications are affected by cell performance, temperature range, products, etc. The followings are the examples of fuel cells currently under development [15, 16].

2.2.1 Polymer Electrolyte Membrane Fuel Cells (PEMFCs)

Polymer electrolyte membrane fuel cells (as shown in Figure 2.2) are also called proton exchange membrane fuel cells. PEMFCs use solid polymer as an electrolyte and platinum catalyst on carbon electrodes. Hydrogen and oxygen are fed as reactants at anode and cathode, and then water is produced at cathode. Unfortunately, platinum is extremely sensitive to carbon monoxide (CO) poisoning; in case where hydrogen is produced from hydrocarbon fuel, CO must be eliminated or reduced in fuel gas.

PEMFCs show high power density, low weight and volume. They are used for transportation such as cars, busses and stationary applications, but their problem is hydrogen storage. Hydrogen has low energy density; hence, to store enough hydrogen onboard for vehicles to travel as long as gasoline does before refueling, hydrogen must be stored in the pressurized tank. Higher density fuel such as methanol, gasoline, natural gas and LPG can be used for fuel instead of pure hydrogen, but the reforming apparatus must be added to convert liquid fuel to hydrogen. This increases cost and maintenance requirement for the car.

2.2.2 Direct Methanol Fuel Cells (DMFCs)

Direct methanol fuel cells use methanol as fuel. They use solid polymer membrane, the same kind as PEMFCs, as electrolyte. Methanol is mixed with steam and fed directly to the cells anode, and converted to hydrogen within the cells. Methanol has a higher energy density than hydrogen but less than gasoline and diesel fuel, therefore DMFCs do not have many storage problems. The major problems of DMFCs are high

methanol permeability rate and CO poisoning effect on electrode. These problems cause loss of fuel efficiency and increase cost.
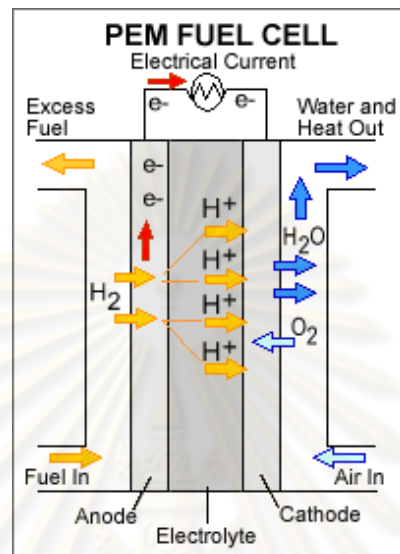
Figure 2.2 Polymer Electrolyte Membrane Fuel Cells (PEMFCs) [15]

2.2.3 Alkaline Fuel Cells (AFCs)

Alkaline fuel cells (as shown in Figure 2.3) are one of the first types of fuel cells technology developed. They were the first type used in the U.S. space program to produce electrical energy and water on space craft. Potassium hydroxide solution is used as the electrolyte and non-precious metals are used as a catalyst at anode and cathode. AFCs operate at high temperature range (100 – 250 °C) and can also be operated at low temperature range (23 – 70 °C).

Carbon dioxide can affect the AFCs performance even the small amount leading to reduced cells performance. Thus hydrogen and oxygen are necessary to be purified before being fed to the cells. The purification process adds cost. The life time of AFCs stacks before needed maintenance is 8,000 operating hours, but the needed operating time for the large scale applications is at least 40,000 hours [15].
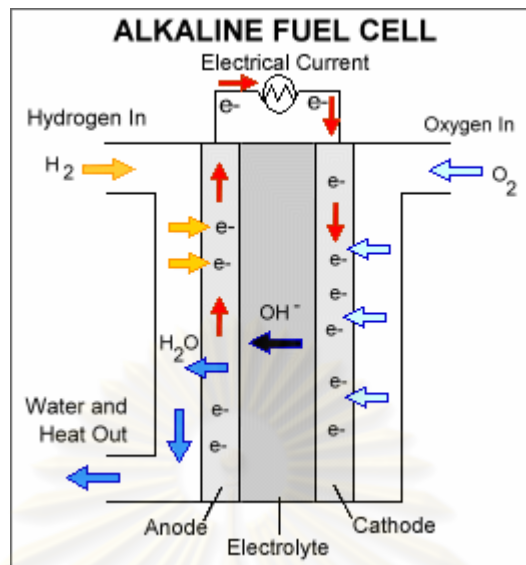
Figure 2.3 Alkaline Fuel Cells (AFCs) [15]

2.2.4 Phosphoric Acid Fuel Cells (PAFCs)

Phosphoric acid fuel cells (as shown in Figure 2.4) are the first of modern fuel cells used commercially. They are used for stationary power generation and to power large vehicles. The electrolyte of phosphoric acid fuel cells is liquid phosphoric acid and the electrodes are porous carbon containing platinum catalyst.

The platinum catalyst electrode at anode of PAFCs are extremely affected or poisoned by carbon monoxide and carbon dioxide from impurities in the fossil fuels. The efficiency of this fuel cell is decreased from 85% to 37% when contaminated hydrogen is used. PAFCs have efficiency lower than other fuel cells because of their high weight and volume. They are also expensive due to the cost of platinum catalyst [15].

2.2.5 Molten Carbonate Fuel Cells (MCFCs)

Molten carbonate fuel cells use a molten carbonate salt mixture suspended in a porous chemically inert ceramic lithium aluminum oxide ($LiAlO_2$) matrix as an electrolyte (as shown in Figure 2.5). These fuel cells are developed for natural gas and coal-based power plants for electrical utility, industrial and military applications.
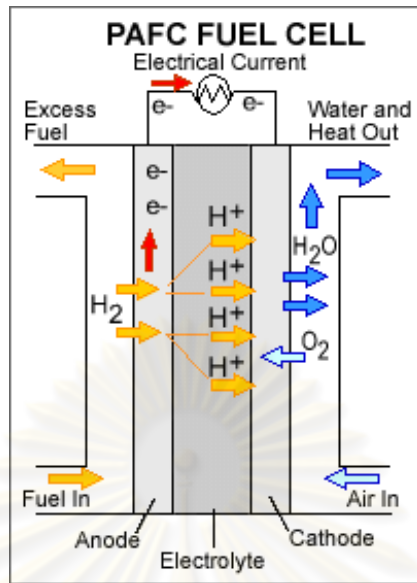
Figure 2.4 Phosphoric Acid Fuel Cells (PAFCs) [15]
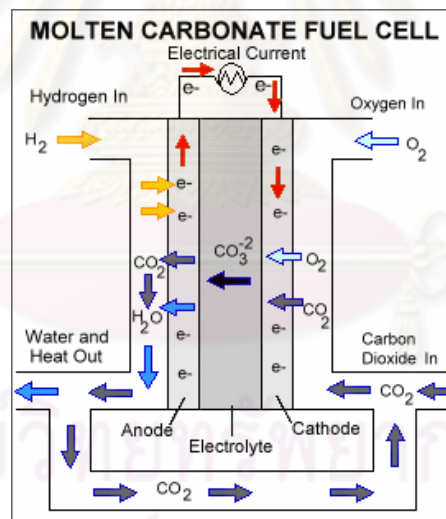
Figure 2.5 Molten Carbonate Fuel Cells (MCFCs) [15]

MCFCs can convert hydrocarbon fuel to hydrogen within the cells themselves, called internal reforming, because they operate at high temperature (650 °C). The advantage of these fuel cells is the waste heat from the process can be used. This reason is why MCFCs have high efficiency and low cost.

Carbon monoxide and carbon dioxide are not poison on molten carbonate fuel cells; instead these fuel cells can use carbon dioxide as fuel. They can even use gases from reforming of coal because they are more resistant to impurities such as sulphur and particulates. Disadvantage of MCFCs is short life time because of high operating temperature and the corrosive electrolyte.

2.2.6 Solid Oxide Fuel Cells (SOFCs)

Solid oxide fuel cells use non-porous ceramic compound as the electrolyte (as shown in Figure 2.6). Their efficiencies are around 50% – 60% for converting fuel to electricity, and the efficiency could be up to 80% – 85% when used in applications designed to capture and utilize the waste heat i.e. co-generation power plant. SOFCs operate at very high temperature (around 1,000 °C). They can use various fuels and the operation cost can be reduced by adding reformer to the system.

SOFCs are sulfur-resistant fuel cells, and they can not be poisoned by carbon monoxide. Thus, SOFCs can use gases from coal. However, solid oxide fuel cells have disadvantages due to very high operating temperature such as slow startup and they require heat insulator. Their applications are suitable for stationary supply but not for use in vehicles. New membrane with low cost and high durability materials must be developed for SOFCs.
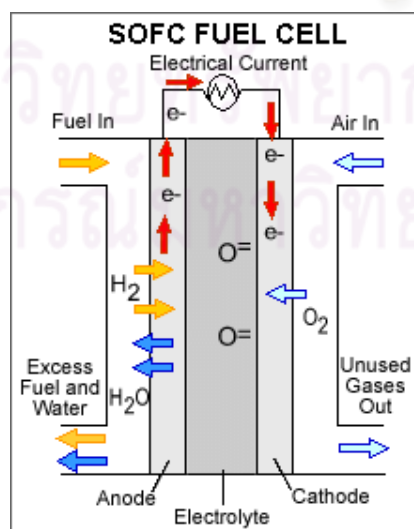
Figure 2.6 Solid Oxide Fuel Cells (SOFCs) [15]

Table 2.1 listed some important characteristics of different types of fuel cells.

Table 2.1 Types of Fuel Cells and Their Characteristics [15-17]

Fuel Cell Type	Proton Exchange Membrane (PEMFC)	Direct Methanol (DMFC)	Alkaline (AFC)	Phosphoric Acid (PAFC)	Molten Carbonate (MCFC)	Solid Oxide (SOFC)
Anode Gas	H_2	Methanol solution	H_2	H_2	H_2, Methane	H_2, Methane
Cathode Gas	Air, O_2	Air, O_2	Pure O_2	Air, O_2	Air, O_2	Air, O_2
Mobile Ion	H^+	H^+	OH^-	H^+	CO_3^{2-}	O^{2-}
Efficiency (%)	35 – 60	35 – 40	50 – 70	35 – 50	40 – 55	45 – 60
Temp. (°C)	50 – 100	30 – 80	50 - 200	~ 220	~ 650	600 - 1000
Power Density (kW/m^2)	3.8 – 2.6	2.5 – 1.5	0.7 – 8.1	0.8 – 1.9	0.1 – 1.5	1.5 – 2.6
Start-up Time	sec – min	sec – min	min	hours	hours	hours
Electrolyte	Solid polymer membrane	Solid polymer membrane	Potassium hydroxide	Phosphoric acid	Alkali carbonates	Ceramic oxide

There are advantages and disadvantages of fuel cells [18]:

Advantages

- Fuel cell, which uses hydrogen as fuel, emits non-pollution gases and no noise.

- Operate at low temperature and require little warm up time.

- Fuel cell can be refueled, which is faster than charging battery.

- Fuel cell shows high performance. Its efficiency is higher than other thermal engines, and does not exhibit a sharp drop when power plant size decreases as shown in Figure 2.7.
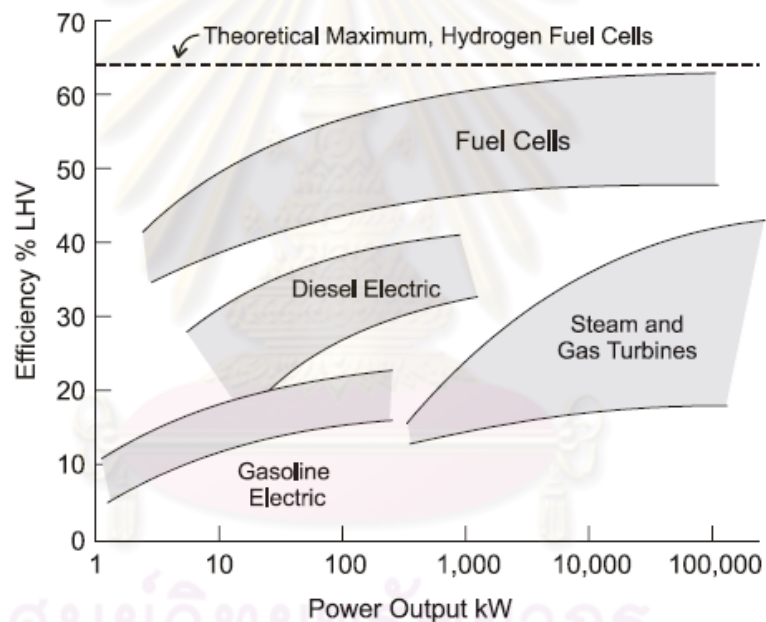
Figure 2.7 Efficiency Comparisons [18]

Disadvantages

- Hydrogen fuel is difficult to manufacture and store.

- The contamination of fuel can reduce the fuel cell performance.

- The platinum catalyst which used in proton exchange membrane fuel cell is very expensive.

- The hydrogen refueling station is not widely established.

2.3 Proton Exchange Membrane

Polymer electrolyte membrane or proton exchange membrane fuel cells (PEMFCs) are one of several kinds of fuel cells but they are typically used in vehicles. Single cell of proton exchange membrane consists of proton conducting membrane as electrolyte, such as Nafion[®] (perfluorosulphonic acid) which has high proton conductivity. The electrolyte is contained between two platinum-impregnated electrodes (anode and cathode). Hydrogen is fed at the anode side and oxidized to protons (hydrogen ions) and electrons by platinum catalyst. The cell operates at temperature around 70 – 80 °C. Electrons move pass through external circuit, to create electricity, and protons diffuse through the membrane. Protons and electrons react with oxygen from air to produce water at cathode.

Oxidation reaction at the anode

$$H_2 \longrightarrow 2H^+ + 2e^-$$

Reduction reaction at the cathode

$$\frac{1}{2} O_2 + 2H^+ + 2e^- \longrightarrow H_2O$$
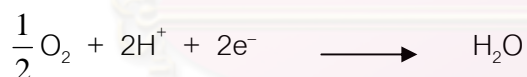
The technology of proton exchange membranes was developed in 1940s [17]. The organic ion exchange membranes or ionomers are believed to be suitable membranes for general use. The development of fluorocarbon based ionomers is one of the most important researches in the field of ionomers. It consists of a linear perfluorinated backbone with side chains that are terminated with ionic groups. Commercially available ionomer are Nafion[®] membrane (DuPont, USA), the Dow membrane (Dow Chemicals, USA), Flemion[®] (Asahi Glass Co., Japan) and Aciplex-S[®] (Asahi Chemical Industry Co., Japan).

Polymer electrolyte membrane (proton exchange membrane) is one of the important parts of polymer electrolyte membrane fuel cell. The membrane must conduct

protons (hydrogen ions) but not electrons. The polymer electrolyte membrane separates hydrogen and oxygen to different side to prevent the reaction to occur directly. Electrons pass through external circuit only because polymer electrolyte membrane is an electric insulator.

In fuel cell, the membrane may be contaminated by other metal ions which affect the proton conductivity of the membrane. Metal ions compete with hydrogen ions to move through the membrane. Therefore, the performance of the cell decreases.

Nafion[®] membrane (DuPont) has been widely used as proton exchange membrane for fuel cell applications. This polymer membrane is based on a polytetrafluoroethylene (PTFE) backbone and has perfluorovinyl ether pendant side chains, with the sulfonate groups at the end. Nafion[®] has good ion selectivity, proton conductivity and chemical resistance. The equivalent weight of Nafion[®] membrane has been commercially available in 900, 1100, 1200, and other equivalent weights. The chemical structure of Nafion[®] is shown in Figure 2.8. Typical properties of Nafion[®] membrane are shown in Table 2.2.
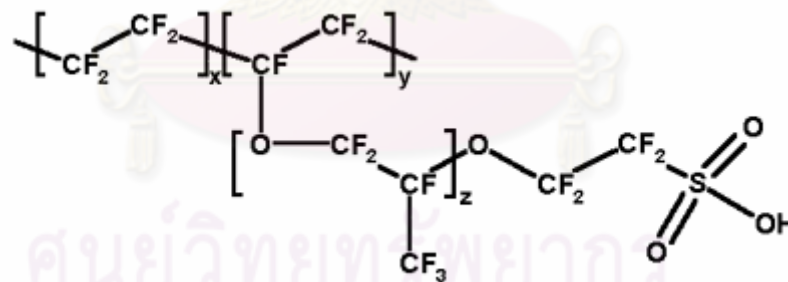
Figure 2.8 Structural Formula of Nafion[®] Polymer [19]

Jalani [17] reported that Nafion[®] membranes are produced by forming the sulfonyl fluoride polymer into sheets and then hydrolyzing to the sulfonate. Once the sulfonate is formed, the membranes swell in various organic solvents, but the material is extremely insoluble. Based on the insolubility and inertness of fluorocarbons, Nafion[®] is normally thought to be a very stable and robust material. Under pressure and

temperature, the sulfonate polymer can be suspended in mixed solvents; these suspensions are used to modify electrodes and are often used in the formation of membrane electrode assemblies of PEMFCs to control wetting.

Table 2.2 Typical Properties of Nafion® Membrane 115 [17]

Physical Properties	Typical Value	Test Method
Tensile Modulus (MPa)		
50% RH, 23 °C	249	ASTM D882
Water soaked, 23 °C	114	ASTM D882
Tensile Strength, max (MPa)		
50% RH, 23 °C	43	ASTM D882
Water soaked, 23 °C	34	ASTM D882
Elongation at Break (%)		
50% RH, 23 °C	225	ASTM D882
Water soaked, 23 °C	200	ASTM D882
Specific Gravity	1.98	
Conductivity (S/cm)	0.1 minimum	*
Total Acid Capacity (meq/g)	0.95 to 1.01	**
Water Uptake (%)	38	***

Note: * Membrane conditioned in 100 °C water for 1 hr. Measurement cell is submerged in 25 °C D.I. water during experiment. Membrane impedance (real) is taken at zero imaginary impedance.

** A base titration procedure measures the equivalents of sulfonic acid in the polymer, and uses the measurement to calculate the acid capacity or equivalent weight of the membrane.

*** Water uptake from dry membrane to water soaked at 100 °C for 1 hr (dry weight basis).

The transfer of protons in solid polymer electrolyte membrane, e.g. Nafion[®], depends on water content of the membrane. Some of the water, which is tightly bound to the sulfonate group, is called chemically bound water. These are less hydrogen bonded than in the bulk water because of the less water-water contacts. The bulk water is described as physically bound water. Away from the pore surface, in the central region of the pore, the water is present as bulk water. Figure 2.9 shows the various proton transport mechanisms; 1) proton hopping along pore surface (Figure 2.9a), i.e., surface diffusion, in an interfacial zone of roughly the thickness of water molecule (3-5 Å), the transfer of proton would take place through the tightly bound water molecules along the array of sulfonate group; 2) the structural diffusion in pore bulk (Figure 2.9b), the transfer of proton in the center of the pore would follow the transfer in bulk water; 3) vehicular mechanism (Figure 2.9c), proton rides along with the diffusing H_2O (or vehicle) as H_3O^+. On the other hand, in structural diffusion, the proton simply hops from one solvent to the adjacent one, without vehicular mechanism. As the membrane becomes saturated, the size of pore increases and this will increase the bulk-like portion of water, leading bulk-like transfer that give high rate of proton transfer in the middle of pores [17]. However, absorbed water also affects the mechanical properties of the membrane by acting as a plasticizer, lowering the T_g and modulus of the membrane. Careful control of water uptake is critical for reducing adverse effects of swelling and degradation of the mechanical properties of the membrane in humid environments, as well as inducing stresses between the membrane and the electrodes [19].
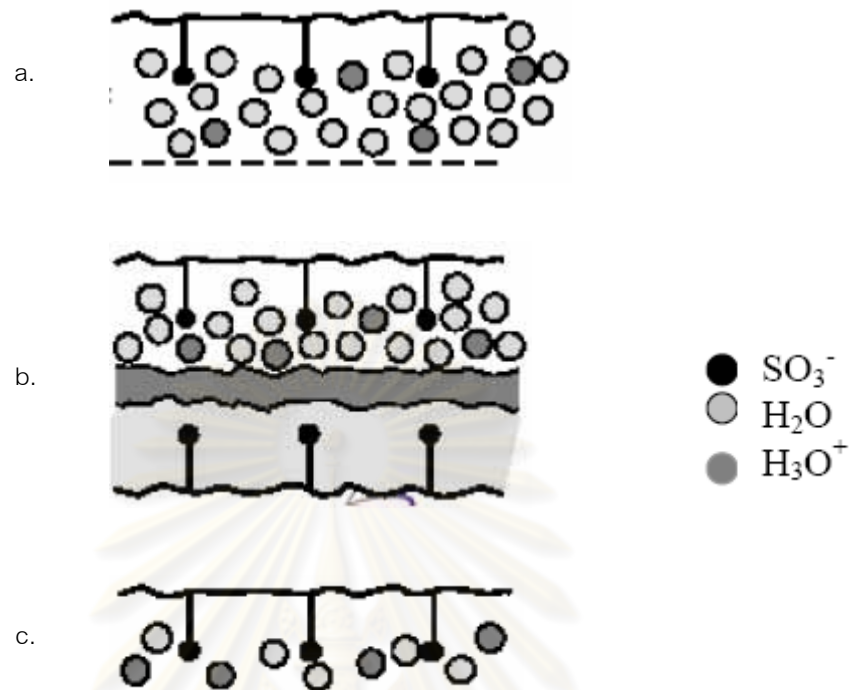
Figure 2.9 A Simplified Picture of Structure and Proton Transfer in Nafion[®] in Fully Hydrated State: (a) Proton Transfer in Pore Surface; (b) Proton Transfer in Pore Bulk; (c) Proton Transfer by H_3O^+ [17]

2.4 Clay

In general the term clay implies a natural, earthly, fine-grained material which develops plasticity when mixed with a limited amount of water. Chemical analyses of clays show them to be composed essentially of silica, alumina, and water, frequently with appreciable quantities of iron, alkalies, and alkaline earths [20].

Clay minerals are a group of hydrous layered magnesium or alumino-silicates (phyllosilicates). Each magnesium-phyllosilicate or alumino-phyllosilicate is essentially composed of two types of sheet, octahedral and tetrahedral sheets. The tetrahedral sheet is a continuous linkage of SiO_4 tetrahedrons; through sharing of three oxygen atoms with three adjacent tetrahedrons that produces a sheet with a planar network in the form of a hexagonal network. The octahedral layer is obtained through condensation

of single $Mg(OH)_6^{4-}$ or $Al(OH)_6^{3-}$ octahedron. Each oxygen atom is shared by three octahedron, but two octahedrons can share only two neighboring O atoms that can be arranged to form a hexagonal network [21]. The two major types of clay minerals are 1:1 and 2:1 type minerals [22].

1:1 type minerals

The 1:1 clay-mineral type consists of one tetrahedral sheet and one octahedral sheet. These two sheets are approximately 0.7 nm thick as shown in Figure 2.10. A kaolinite mineral is one of the 1:1 type minerals.
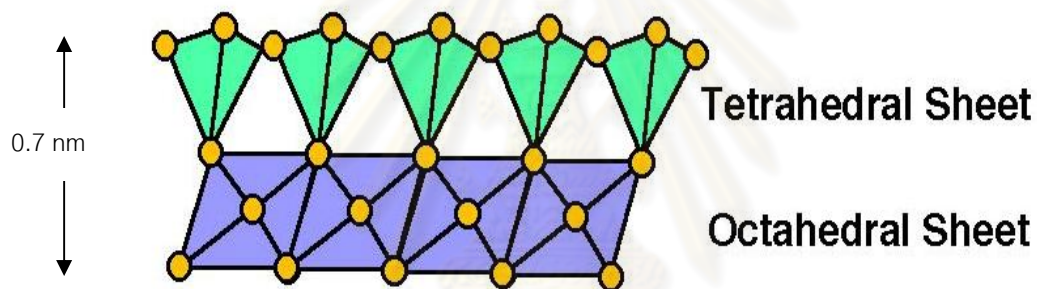
Figure 2.10 Type 1:1 Clay [23]

2:1 type minerals

The three sheet or 2:1 layer lattice silicates consist of two silica tetrahedral sheets between which is an octahedral sheet. These three sheets form a layer approximately 1 nm thick as shown in Figure 2.11. Smectite, vermiculite, and illite are examples of the 2:1 type clay. The properties of clay minerals are shown in Table 2.3.
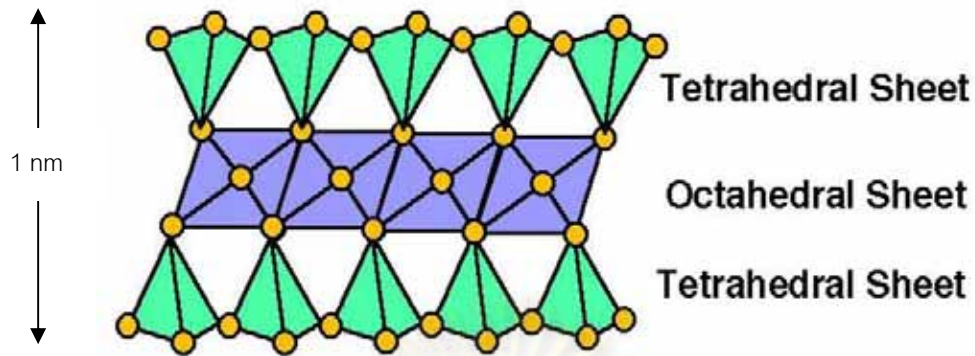
Figure 2.11 Type 2:1 Clay [23]

Table 2.3 Summary of Properties of Different Clay Type [22]

Type	Size	Surface Area (m^2/g)		Interlayer	Cation Sorption
	(µm)	External	Internal	Spacing (nm)	(meq/100g)
Kaolinite	0.1 - 5.0	10 - 50	-	0.7	5 – 15
Smectite	< 1.0	70 - 150	500 – 700	1.0 - 2.0	85 – 100
Vermiculite	0.1 - 5.0	50 – 100	450 – 600	1.0 – 1.4	100 – 120
Illite	0.1 – 2.0	50 – 100	5 – 100	1.0	15 – 40

2.4.1 Montmorillonite

Montmorillonite has the widest acceptability for use in polymer. It is a type of smectite clay and is a layered structure with aluminum octahedron sandwiched between two layers of silicon tetrahedron. Each layered sheet is slightly less than 1 nm thin, with surface dimensions extending to about 1 µm or 1,000 nm. The aspect ratio is about 1,000 to 1 and the surface area is in the range of 750 m^2/g. The molecular structure of 2:1 layered silicate is shown in Figure 2.12.
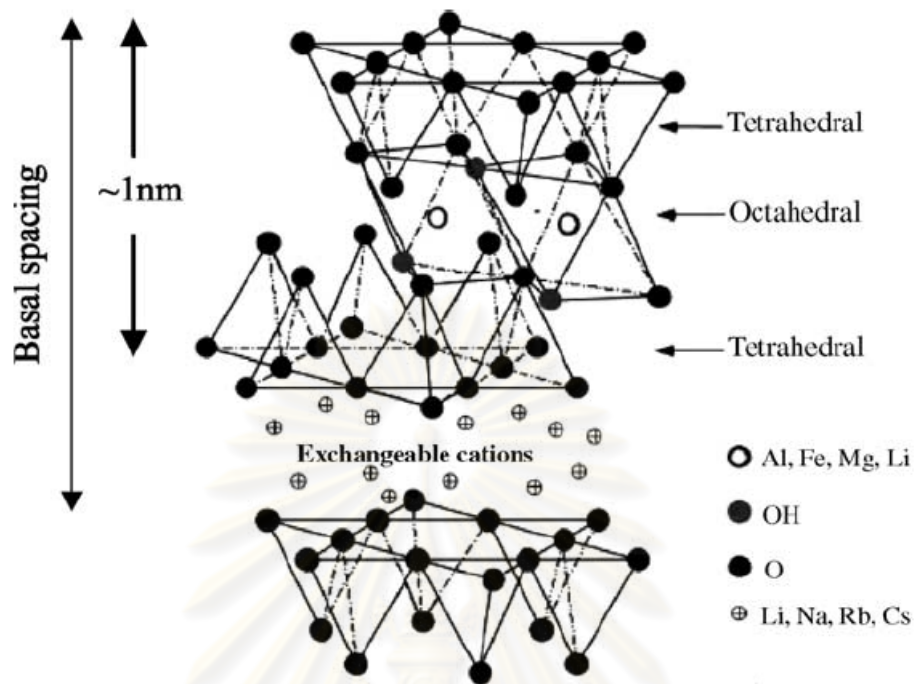
Figure 2.12 Structure of 2:1 phyllosilicates [24]

Montmorillonite has a low thermal expansion coefficient and a high gas barrier property. Stacking of this structure leads to a regular weak dipolar or van der Waals interaction between the layers. Isomorphic substitution in each layer generates negative charges that are counterbalanced by hydrated sodium or potassium ions residing in the interlayer spaces. Due to this special characteristic, montmorillonite can be easily dispersed in water resulting in a stable colloid. Typically, the natural montmorillonite is too hydrophilic to disperse in an organic matrix. Its dispersibility can be improved to make it useful by ion exchange with an organic cation molecule, such as cationic surfactant, onto its surface [22]. In addition, the interlayer ions can be exchanged with ions in surrounding aqueous solution. Large organic molecules can be adsorbed. When water or molecules are adsorbed, the structure swells. This process is reversible and, in a dry atmosphere or during heating, both water and hydrated cation leave the structure of montmorillonites, causing the crystals to decrease in volume [25].

2.5 Nanocomposites

Nanocomposite refers to the two phases in system, one phase is polymer or matrix, and another phase is filler that has nanometer size (10^{-9} m) at least in one dimension. Generally, layered silicates have layer thickness about 1 nm and a very high aspect ratio (e.g. 10 – 1,000). A few weight percent of layered silicates that are properly dispersed throughout the polymer matrix thus create much higher surface area for polymer/filler interaction as compared to conventional composites [24]. In addition, nanocomposites can improve several properties such as mechanical, barrier and thermal properties because of their unique phase morphology and improved interfacial properties [21]. Three different types of polymer layered silicate are achievable as shown in Figure 2.13 [21, 22]:

i) Conventional composite composes of silicate tactoids with the silicate layers aggregated in the unintercalated form. Consequently, discrete phases usually take place because of no penetration of polymer molecules into layer silicate phase resulting in poor mechanical properties of composite materials.

ii) Intercalated nanocomposite consists of a regular insertion of polymer in between silicate layers. The intercalated type of polymer-clay hybrid has been touted to have highly extended single chains confined between the clay sheets, within the gallery regions. The clay sheets retain a well ordered, periodic, stacked structure.

iii) Exfoliated or delaminated nanocomposite which is formed when the silicate nanolayers are individually dispersed in the continuous polymer matrix and exhibit greater phase homogeneity than intercalated nanocomposite. In this case the sheets have lost their stacked orientation, so that the exfoliated nanolayers contribute fully to interfacial interactions with the polymer matrix.
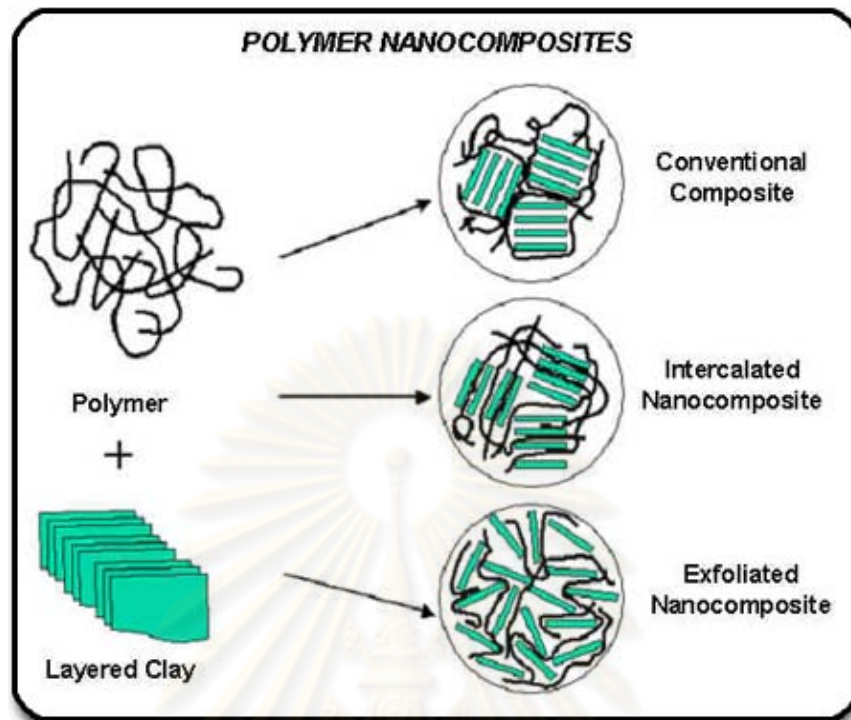
Figure 2.13 Three Types of Polymer/Clay Composite [26]

There are three methods to synthesize polymer/layered silicate nanocomposites:

i) Direct Mixing (Melt Mixing)

Direct mixing takes advantage of well established polymer processing techniques. Nanocomposites can be sufficiently rapidly processed in a twin-screw extruder. The strategy is to blend a molten thermoplastic with organosilicates in order to optimize the polymer/layered silicate interaction.

ii) Solution Mixing

Some of the limitations of melt-mixing can be overcome if both the polymer and the nanoparticles are dissolved or dispersed in solution. This allows modification of the particle surface without drying, which reduces particle agglomeration. The nanoparticle/polymer solution can then be cast into a solid, or the nanoparticle/polymer can be isolated from solution by solvent evaporation or precipitation. After evaporation of solvent, an intercalated nanocomposite is obtained.

iii) In-Situ Polymerization

Another method is in-situ polymerization. Here, nanoscale particles are dispersed in the monomer or monomer solution, and the resulting mixture is polymerized by standard polymerization methods.

In addition to the effect of size in particle properties, the small size of the fillers leads to an exceptionally large interfacial area in the composites. The interface controls the degree of interaction between the filler and the polymer and thus controls the properties. Therefore, the greatest challenge in developing polymer nanocomposites may be learning to control the interface. Once the organoclay is swollen in the monomer, the curing agent is added; in favorable cases exfloliation occurs.

2.6 Mechanical Property

The tensile test is popular since the properties obtained could be applied to design different components. The tensile test measures the resistance of a material to a static or slowly applied force.

Figure 2.14 shows qualitatively the stress (σ)-strain (ε) curves for a typical (a) metal, (b) thermoplastic material, (c) elastomer, and (d) ceramic (or glass), all under relatively small strain rates. The scales in this figure are qualitative and different for each material. In practice, the actual magnitude of stresses and strains will be very different. The thermoplastic material is assumed to be above its glass transition temperature (T_g). Metallic materials are assumed to be at room temperature. Metallic and thermoplastic materials show an initial elastic region followed by a non-linear plastic region. A separate curve for elastomers (e.g. rubber or silicones) is also included since the behavior of these materials is different from other polymeric materials. For elastomers, a large portion of the deformation is elastic and non-linear. On the other hand, ceramics and glasses show only a linear elastic region and almost no plastic deformation at room temperature [27].

(a) Metal

(b) Thermoplastic material above T$_g$

(c) Elastomer

(d) Ceramics, glasses, and concrete
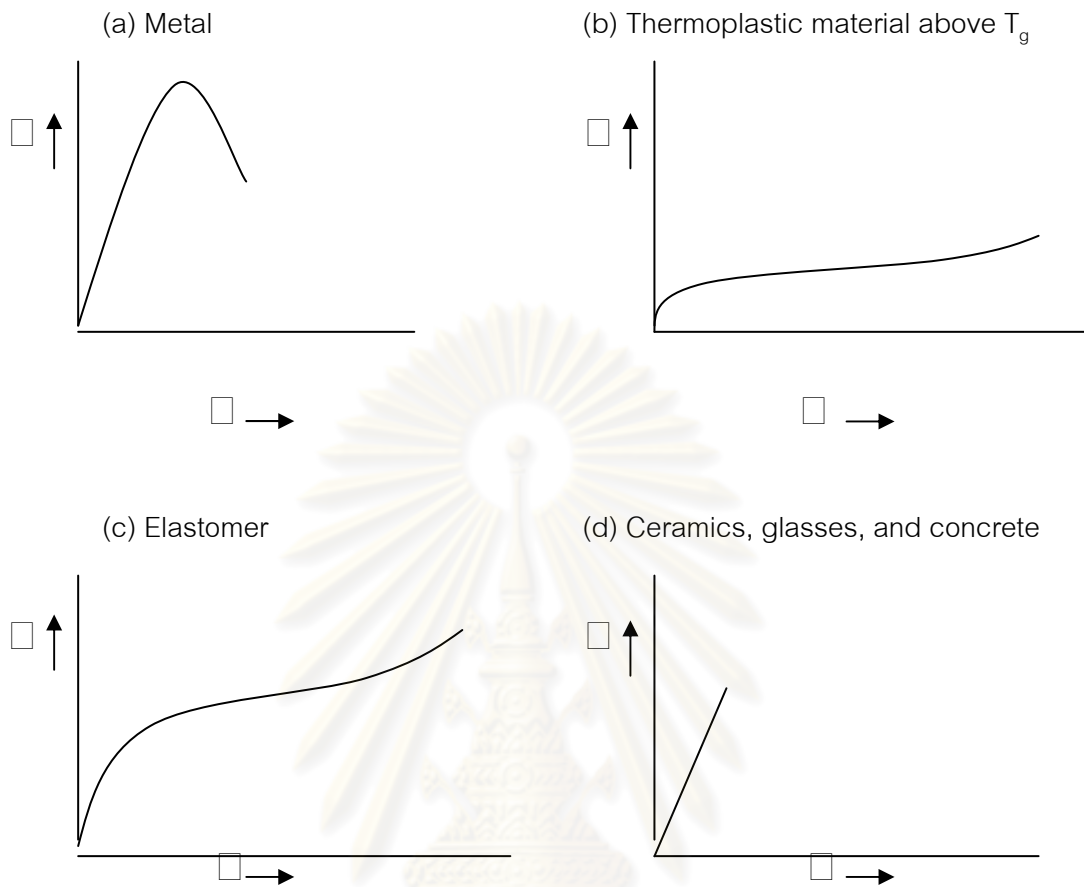
Figure 2.14 Tensile stress (   )-strain (   ) curve for different materials [27]

2.6.1 Stress

The external forces applied to a component result in stresses within the material. A stress is a measure of the force in a component relative to the cross-sectional area over which the force is applied. Stress is measured in force per unit area, for example, lb/in^2 or N/m^2 (Pascal, Pa) [28].

$$\sigma \;=\; \frac{F}{A}$$

(2.1)

Where σ is the stress, F is the force, and A is the area.

2.6.2 Strain

Stress usually causes material to deform in length. The change in length as it relates to the original length is call strain. Hence, strain is denoted as [28].

$$\varepsilon \; = \; \frac{\delta}{L}$$

(2.2)

Where L is the original length and δ is the change in length that occurs when the material is pulled by force F.

In terms of stress and strain, Hooke's law may be rewritten as

$$\sigma \; = \; E \, \varepsilon$$

(2.3)

Where E is a constant of proportionality referred to as Young's modulus or the elastic modulus. The modulus of elasticity is of crucial importance in materials selection. It determines the elastic deflection of a structure member under load. Polymers often have very low elastic moduli compared with metals and ceramics.

2.6.3 Tensile Test

The test sample is mounted in a tensile machine using grippers or jaws. One jaw is fixed to the base of the testing machine, and the other is affixed to a movable crosshead. The tensile stress is calculated by dividing the force by the original cross-sectional area. The strain is calculated by dividing the change in length of the sample by the original length. Instrumentation such as a computer then calculates a stress-strain graph. Typical stress-strain curve of material is shown in Figure 2.15.

During the early stages of the test, the sample will behave elastically. That is, if the crosshead were stopped, the sample will return to its original length. As the test continues, the stress in the sample increases, and the length of the sample within the

gauge region becomes longer. The stress-strain curve is approximately linear, and the slope of that curve is the elastic modulus. Materials that exhibit a linear stress-strain curve in the elastic range are said to be Hookean [28].
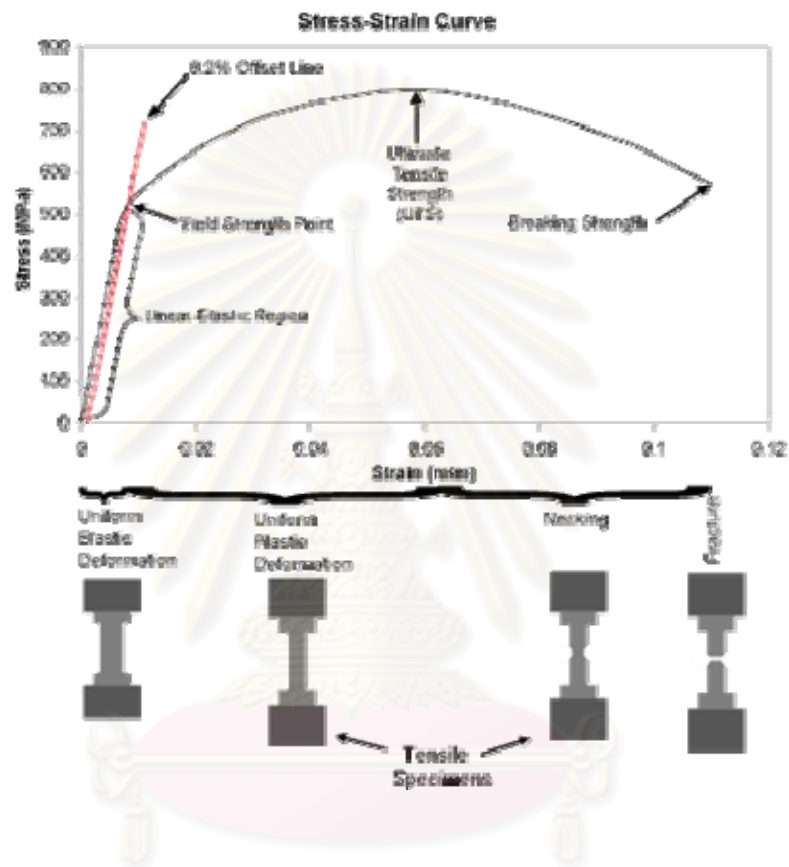
Figure 2.15 Stress-Strain Curve [29]

The modulus of elasticity is the slope of the linear portion of the stress-strain curve and may be calculated through the following equation,

$$E = \frac{\Delta stress}{\Delta strain} \qquad (2.4)$$

where $\Delta stress$ and $\Delta strain$ are the respective increments in stress and strain on the linear portion of the stress-strain curve as shown in Figure 2.16.
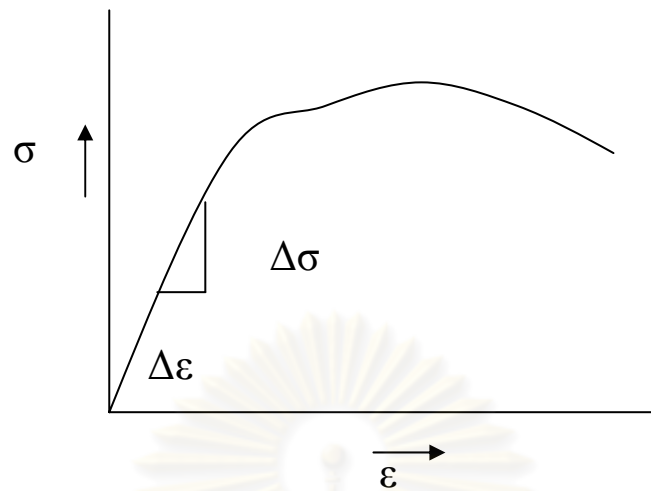
Figure 2.16 Example of Stress-Strain Curve for Determining Modulus of Elasticity

Over a range of stresses, the stress-strain curve begins to deviate from linearity, even though it is still in the elastic range. This transition to nonlinearity occurs at a point referred to as the proportional limit. Below this point, the material exhibits Hookean elastic behavior. In some instances, the material may still behave elastically for a small increment of strain above the proportional limit although in a nonlinear, non-Hookean manner.

As the stress continues to increase in the sample, the sample continues to elongate until it finally reaches a point where some permanent plastic deformation occurs. If the sample were unloaded at this point, the specimen would be slightly longer than its original length. This permanent increase in length is referred to as plastic deformation. The point at which the deformation of the material changes from elastic deformation to plastic deformation is referred to as the elastic limit or the yield point. Because the yield point is difficult to determine precisely, engineers often consider the yield point to occur at an offset strain of 0.2% (for metallic materials). Testing standards, such as ASTM, also designate the stress at 0.2% offset strain as the yield stress or yield strength of the material. Yield strength is typically measured in psi or Pa.

As the crosshead in the tensile tester continues to elongate the sample, the tensile force in the sample continues to increase in a nonlinear manner as shown in

Figure 2.15. Simultaneously, the cross-sectional area of reduced section of the test sample begins to decrease as the sample length increases. Initially, this reduction in cross-sectional area occurs uniformly over the reduced section of the sample. As the tester continues to pull the sample, two competing effects occur. The material continues to harden and gets stronger; however, at the same time the cross-sectional area of the sample begins to rapidly decrease, reducing the load-carrying capacity of the test specimen. The force curve reaches a peak and then begins to drop off with continued extension. The stress calculated at this peak load is called the ultimate tensile strength of the material. Before the ultimate tensile stress is reached, the rate of work hardening the material increases faster than the reduction in cross-sectional area. At the ultimate tensile stress, the rate of cross-sectional area reduction occurs faster than the work hardening rate, so the load-carrying capacity of the specimen decreases and the curve begins to drop off. Typically, at the ultimate tensile stress point, the reduction in cross-sectional area occurs in a pronounced, localized spot on the test sample. This localized reduction in area is known as necking. As the test proceeds, ultimately the sample fractures into two halves.

Once the sample fractures, it is removed from the tensile testing machine and two measurements are made:

a) The fractured sample is reassembled as best as possible and the final length of the gauge area is measured.

b) The final diameter of the necked down portion of the sample is also measured.

These two measurements are used to assess the ductility of the material. Ductility, a measure of ability of a material to be stretched or drawn, is typically reported as percent elongation or percent reduction in area. The percent elongation is a ratio of the increase in length incurred in the sample up to the point of fracture relative to the initial length of the sample. Percent elongation is calculated by the following equation,

$$\text{Percent elongation} = \frac{\text{final length} - \text{initial length}}{\text{initial length}} \times 100 \qquad (2.5)$$

The higher the percent elongation, the material is more ductile and formable. When comparing the ductility of materials, always verify that the percent elongation data are based on the same gauge length.

Percent reduction in area is measured by comparing the cross-sectional areas of the test specimen before and after fracture (usually done with cylindrical tensile specimens). To measure the final cross section of the sample, the fractured sample is assembled as best as possible and the final diameter in the necked-down region is measured (the initial diameter must also be measured before testing). Percent reduction in area is calculated by the following equation,

$$\text{Percent reduction in area} = \frac{\text{initial area} - \text{final area}}{\text{initial area}} \times 100 \qquad (2.6)$$

According to ASTM D 882 for tensile properties of thin plastic sheeting, ten rectangular specimens, five for normal and five for parallel with the principal axis of anisotropy, are tested. Figure 2.17 shows the standard shape and the dimensions of the test specimen. The speed of testing is calculated from the required initial strain rate as specified in Table 2.4. The rate of grip separation may be determined for the purpose of those test methods from the initial strain rate as follows,

$$A = BC \qquad (2.7)$$

Where: A = rate of grip separation, mm (or in.)/min,

                  B = initial distance between grips, mm (or in.), and

                  C = initial strain rate, mm/mm • min (or in./in. • min)

Table 2.4 Speed of testing

Percent Elongation at Break	Initial Strain Rate, mm/mm • min (or in./in. • min)
Modulus of Elasticity Determination	
	0.1
Determinations other than Elastic Modulus	
Less than 20	0.1
20 to 100	0.5
Greater than 100	10.0
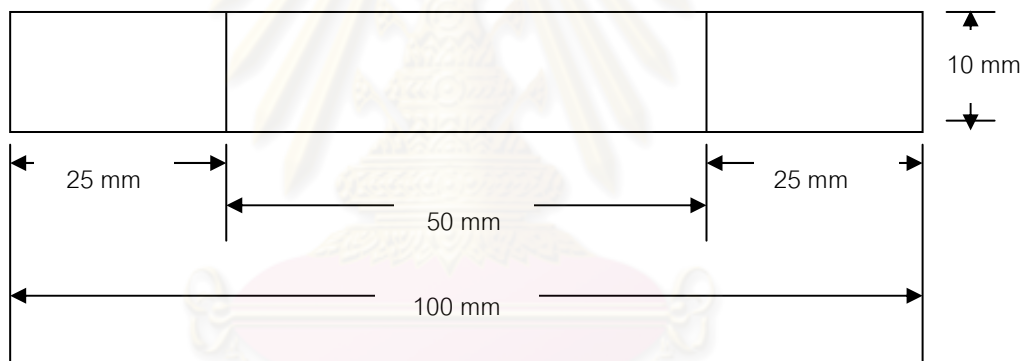
Figure 2.17 Dimension of Test Specimen (ASTM D 882)

2.7 X-Ray Diffraction (XRD)

X-Ray Diffraction (XRD) is the most commonly used technique to characterize the degree of expansion of interlayer spacing of MMT organoclay in a specific polymer. XRD measures the spacing between the ordered crystalline layers of the organoclay by using Bragg's law [30,31],

$$2d \sin \theta = n\lambda \tag{2.8}$$

where d is the spacing between atomic planes in the crystalline phase

λ is the x-ray wavelength

θ is the reflection angle

n is the order of reflection

Bragg's Law can easily be derived by considering the conditions necessary to make the phases of the beams coincide when the incident angle equals the reflecting angle. The rays of the incident beam are always in phase and parallel up to the point at which the top beam strikes the top layer at atom z (Figure 2.18). The second beam continues to the next layer where it is scattered by atom B. The second beam must travel the extra distance AB + BC if the two beams are to continue traveling adjacent and parallel. This extra distance must be an integral (n) multiple of the wavelength (λ) for the phases of the two beams to be the same:
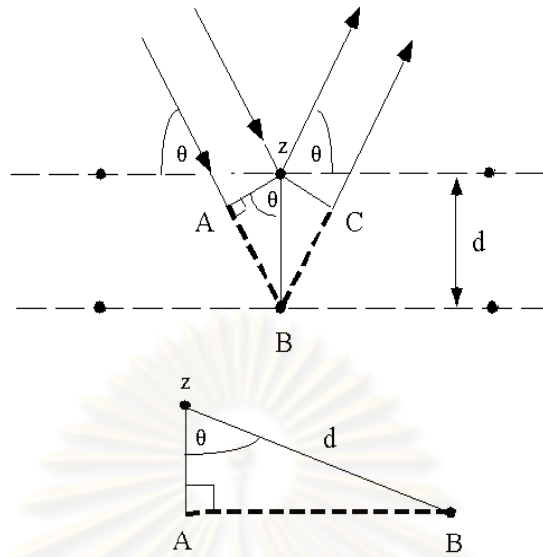
Figure 2.18 Deriving Bragg's Law Using the Reflection Geometry and Applying

Trigonometry [31]

$$n\lambda = AB + BC \tag{2.9}$$

Recognizing d as the hypotenuse of the right triangle ABz, the distance AB is opposite

θ so,

$$AB = d \sin\theta \tag{2.10}$$

Because AB = BC, eq. (3.9) becomes

$$n\lambda = 2AB \tag{2.11}$$

Substituting eq. (3.10) in eq. (3.11) gives

$$2d \sin\theta = n\lambda \tag{2.8}$$

The intensity of the diffracted X-ray is measured as a function of the diffraction angle 2θ and the crystalline phases of the specimen. XRD is nondestructive and does not require elaborate sample preparation which partly explains the wide usage of this technique in materials characterization. Spacing change (increase or decrease) information can be used to determine the type of polymer nanocomposite formed, such as

- Immiscible (no d-spacing change)
- Decomposed/deintercalated (d-spacing decrease)
- Intercalated (d-spacing increase)
- Exfoliated (d-spacing outside of x-ray diffraction, or so expansive and disordered as to give a signal)

However, XRD can be affected by many parameters:

- Sampling (powder vs. solids, alignment of clay platelets)
- Experimental parameters (slit width, count time, angle step rate)
- Layered silicate order (disordered/amorphous materials exhibit no pattern by XRD)
- XRD measures d-spacing, not overall (global) clay dispersion in the sample

2.8 Differential Scanning Calorimetry (DSC)

There are several different modes of thermal analysis described as DSC. DSC is a technique of nonequilibrium calorimetry in which the heat flow into or away from the polymer is measured as a function of temperature or time. Presently available DSC equipment measures the heat flow by maintaining a thermal balance between the reference and sample by changing a current passing through the heaters under the two chambers. For instance, the heating of a sample and reference proceeds at a predetermined rate until heat is emitted or consumed by the sample. If an endothermic occurrence takes place, the temperature of the sample will be less than that of the reference. The circuitry is programmed to give a constant temperature for both the

reference and the sample compartments. Excess current is fed into the sample compartment to raise the temperature to that of the reference. The current necessary to maintain a constant temperature between the sample and reference is recorded. The area under the resulting curve is a direct measure of the heat of the transition.

The advantages of DSC over a good adiabatic calorimeter include speed, low cost, and the ability to use small samples. Sample size can range from 0.5 mg to 10 g. Since the temperature difference is directly proportional to the heat capacity, the curves resemble inverted specific heat curves.

Possible determinations from DSC measurements include the following: (1) heat of transition, (2) heat of reaction, (3) sample purity, (4) phase diagram, (5) specific heat, (6) sample identification, (7) percentage incorporation of a substance, (8) reaction rate, (9) rate of crystallization or melting, (10) solvent retention, and (11) activation energy. Thus, thermocalorimetric analysis can be a useful tool in describing the chemical and physical relationship of a polymer with respect to temperature [33].

For example, as a solid sample melts to a liquid it will require more heat flowing to the sample to increase its temperature at the same rate as the reference. This is due to the absorption of heat by the sample as it undergoes the endothermic phase transition from solid to liquid. Likewise, as the sample undergoes exothermic processes (such as crystallization) less heat is required to raise the sample temperature. By observing the difference in heat flow between the sample and reference, differential scanning calorimeters are able to measure the amount of heat absorbed or released during such transitions. DSC may also be used to observe more subtle phase change, such as glass transition. DSC is widely used in industrial settings as a quality control instrument due to its applicability in evaluating sample purity and for studying polymer curing [33].
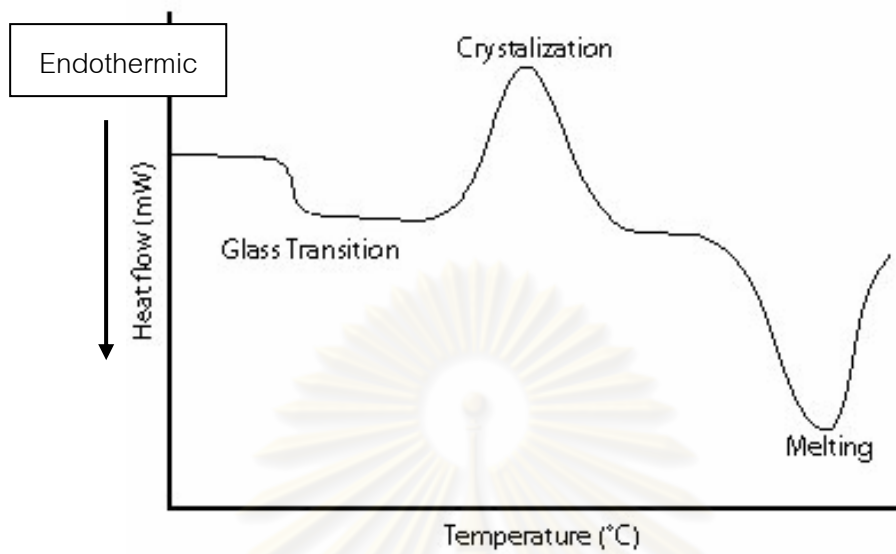
Figure 2.19 A Schematic DSC Curve Demonstrating the Appearance of
Several Common Features [33]

CHAPTER III

LITERATURE REVIEWS

The incorporation of Montmorillonite (MMT) clay into Nafion® matrix were expected to improve the desired properties of proton exchange membrane such as increased mechanical strength, higher thermal stability, decreased methanol permeability, and improved water retention of the membrane.

In 2005, Thomassin et al. [5] studied the effect of dispersion of modified Montmorillonite (m-MMT) with 5 wt% Nafion® by solvent mixing method to form composite membrane. The contents of m-MMT in the mixture were 1, 2, 3 and 4 wt% based on Nafion®. The native sodium Montmorillonite and H-substituted Montmorillonite clay were modified by exchanging the internal counter-ions with behenyl betaine (BHB), 6-aminocaproic acid (ACA), and dimethyloctadecyl (3-sulfopropyl) ammonium hydroxide (DMOSPA), respectively. They found that Montmorillonite clay modified by BHB (Cloisite BHB) could be dispersed in Nafion® matrix better than others, although the nanoclays were not completely exfoliated. In order to improve methanol permeability and ionic conductivity, a 4 wt% Cloisite BHB was the most effective additive into Nafion® membrane. The permeability was decreased by 51% which was almost as high as the 60% decrease observed for completely exfoliated MMT. Moreover, Cloisite BHB was suspected to improve the water retention and the mechanical stability of Nafion® membrane at high temperature.

In 2006, Rhee et al. [7] prepared nanocomposite membranes of surface-sulfonated titanate and Nafion® membrane. They compared the tensile properties of pristine Nafion® 115 membrane and Nafion® composite membrane with additions of 3 wt% of Montmorillonite, TiO_2 P25 and surface-sulfonated titanate, respectively. The results showed that all composite membranes exhibited a large increase in the tensile properties as shown in Figure 3.1. The extent of the improvement of the modulus depended directly upon the morphology and the aspect ratio of the dispersed inorganic

fillers. MMT had a large particle size of micrometer scale and its aspect ratio was over 100:1. TiO_2 P25 has no layered structure and is difficult to be homogeneously dispersed in a nanocomposite membrane. Its impact on the mechanical property of membrane was similar to that of MMT. However, surface-sulfonated titanates with a nanosheet-like morphology showed a more enhanced mechanical strength than MMT or TiO_2 P25 because sulfanated titanate with ca. 0.8 nm interlayer spacing can be easily exfoliated in Nafion[®] matrix.
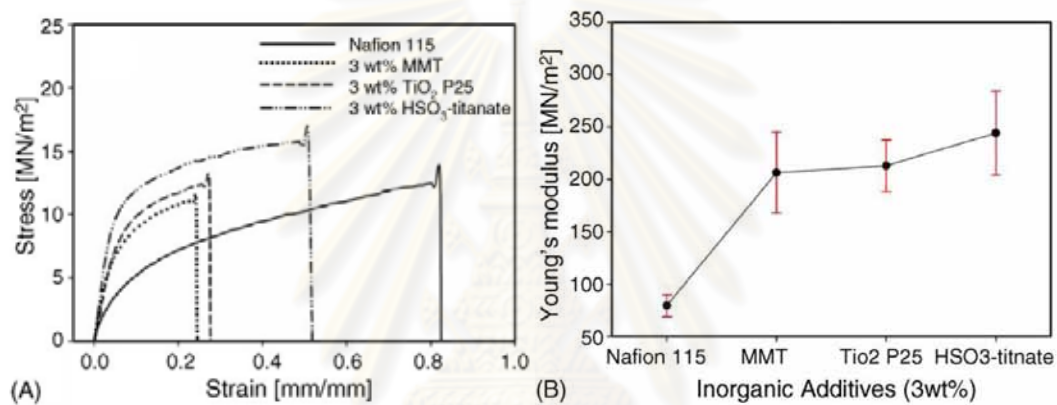
Figure 3.1 Effect of morphology of inorganic fillers:

(A) Stress-strain curve; (B) Young's Modulus [7]

In 2006, Thomassin et al. [8] prepared composite membrane by melt mixing method between Nafion[®] membrane and modified Montmorillonite with required amount of MMT at 1, 2, 3 and 4 wt% based on Nafion[®]. The native MMT was modified using ammonium cations bearing a fluoroalkyl group (Zonyl) and a perfluoroether group (quaternized ammonium perfluoropolyether, PFPE-NR$_3$). They suggested that it was much easier for the organo-modified MMT to interact with the side-chains than with the backbone of the Nafion[®] matrix; therefore, the ammonium that contains a perfluoropolyether segment (MMT-PFPE-NR$_3$) similar to the short side-chains of Nafion[®] has beneficial effect on the filler dispersion. Beyond 2 wt% of addition of MMT-PFPE-NR$_3$ resulted in a decrease of the methanol permeability by approximately 20%. Although the

decrease in ionic conductivity upon addition of native MMT was relatively small, it was significantly larger when MMT was modified by voluminous ammonium cations. The PFPE-NR$_3$ cations were an exception possibly because the compatibility of the cation and the matrix alleviated the problem of the ionic transport. Accordingly, the addition of MMT-PFPE-NR$_3$ is well suited to improve the performance of the Nafion® membranes in line with a decrease of the methanol permeability without deleterious effect on the ionic conductivity.

Satterfield et al. [34] measured the mechanical properties of Nafion® and Nafion®/Titania composite membrane in constrained environments. As functions of the temperature and water content, they found that the membranes that were placed in water at 100 °C for 1 h absorbed almost twice the amount of water as membranes placed in water at 25 °C for 24 h. The elastic modulus of both types of the membranes decreased with increasing temperature. At room temperature, the elastic modulus was around 300 MPa, and it decreased to around 100 MPa at 80 °C. The elastic modulus dropped precipitously to less than 10 MPa above 100 °C. Nafion®/Titania composite membranes had slightly higher elastic moduli. The composite membranes exhibited less strain hardening than Nafion®. They concluded that the decrease in elastic modulus coincided with T$_g$, which has been reported to be 110 °C. Moreover, absorbed water also reduced the elastic modulus; the elastic modulus at 25 °C decreased from 300 to 50 MPa as the water content in the membrane increased.

Corti et al [35] characterized low temperature thermal transitions of Nafion® 117 membranes in water and methanol-water mixtures. They concluded that the desorption of water from the ionic cluster occurred in the temperature range of 100-150 °C, and most of the previous authors called it the glass transition temperature of the ionic cluster. However, they preferred to attribute this peak to the desorption of water from the ionic cluster. The energy involved in this process depends on the interaction energy of water with the ionic species; the temperature of the peak would change with the type of counterions and the water content in the membrane. In the dry Nafion® (acid form) samples, a glass transition temperature was observed at -108 °C. When increasing the

relative humidity to which the samples were exposed, this thermal transition shifted to lower temperature, indicating that water had a slight plasticizing effect on the Nafion[®] membrane. The freezing of water in Nafion[®] membrane containing water-methanol take place at temperatures in range of -10 to -20 °C, being relevant to the operation of direct methanol fuel cells in low temperature environments.

In the same year, Kim et al. [9] reported a new type of sulfonated Montmorillonite (HSO_3-MMT) functionalized with perfluorinated sulfonic acid groups. The organic species bearing the perfluorinated sulfonic acid functional group were grafted on MMT to make filler for organic-inorganic composite proton-conducting membranes. The composite membrane was prepared by solution mixing method by addition of a 5 wt% m-MMT based on Nafion[®] into 5 wt% Nafion[®] solution. The surface functionalization of H^+-MMT was performed by dehydration with 1,4-butane sultone (1,4-BS), 1,3-propane sultone (1,3-PS) and 1,2,2-tri-fluoro-hydroxy-L-trifluomethylethane sulfonic acid sultone (FMES) as sulfonic acid precursors. Their results showed that FMES and 1,3-PS were more efficiently grafted on to the surface of MMT than 1,4-BS. The HSO_3-MMT (FMES) has a lower pH and a higher ion-exchange capacity (IEC) (mmol of sulfonic acid per g of HSO_3-MMT) than the others. The proton conductivities of composite membranes were slightly lower than that of Nafion[®] and the ionic conductivity of Nafion/5 wt% HSO_3-MMT (FMES) composite membranes were higher than those of the other composite membranes; in particular, the value was around 98% of Nafion[®] at 303 K. The difference became more significant at 323 K. Moreover, all composite membranes containing 5 wt% inorganic fillers reduced methanol crossover by 40%, while maintaining comparable ionic conductivity relative to pristine Nafion[®] membrane.

Kim et al. [36] prepared Nafion[®]/S-MMT composite membranes in 2006. The K-10 H^+-MMT was treated with 1,3-propane sultone through refluxing H^+-MMT in toluene to obtain S-MMT. The contents of S-MMT that were loaded in Nafion[®] matrix were 0, 2, 5, 7, and 10 wt%. Their results showed that as the content of S-MMT increased up to 5 wt%, the composite membranes had higher tensile strength value than that of pure Nafion[®] membrane. Then, the tensile strength values decreased with the S-MMT amount over 5

wt%. The elongation at break had the same results. The XRD data indicated that the interfacial area between S-MMT and Nafion[®] matrix did not increase with S-MMT amount. Therefore, S-MMT aggregation particles would become defects in the elongation of samples and deter the expansion of samples. They concluded that the Nafion[®]/S-MMT composite membrane with 5 wt% S-MMT loading amount had a maximum tensile strength and elongation.

In 2007, Lin et al. [10] characterized 5 wt% Nafion[®]/modified Montmorillonite (m-MMT) composite membranes by solution mixing method. The m-MMT was prepared by using poly(oxypropylene)-backboned quaternary ammonium salts (POP) of various molecular weights (M_w = 230, 400 and 2000) as the intercalating agents for MMT. They found that the modified MMT, 1-7 wt% based on Nafion[®], was dispersed in Nafion[®] membrane better than unmodified MMT. The XRD patterns of pristine Nafion[®] and the composite membranes indicated that the sizes of ion channel were changed by introducing m-MMT. It was also suggested that the size of ionic channel were reduced with increasing molecular weight of intercalating agent derived on MMT. However, they observed that MMT-POP 2000 was poorly dispersed in Nafion[®] because MMT-POP 2000 was highly organophilic and had poor interaction with Nafion[®]. The proton conductivity of Nafion[®]/m-MMT composite membrane was lower than that of pristine Nafion[®] membrane due to the proton conductivity of the membrane tended to decrease by adding of MMT. However, they found that 5 wt% MMT-POP 400 could be the optimum level of inorganic in the composite electrolyte membrane. The methanol permeability of the composite membrane decreased dramatically with increasing content of MMT-POP-diamine in the composite membrane. The addition of MMT-POP 400 resulted in a decreasing of methanol permeability by approximately 40%. Although the proton conductivity of Nafion[®]/5 wt% MMT-POP 400 composite membrane was still slightly low but this composite membrane exhibited substantially improved performance by reducing the methanol crossover drastically compared with the pristine Nafion[®] membrane.

In 2007, Zhang et al. [11] studied the interactions between 5 wt% Nafion[®] and Montmorillonite which was modified with protonated dodecylamine. The composite membranes were prepared by solution mixing method, and the contents of m-MMT in the mixture were 3, 5, 8 and 10 wt% based on Nafion[®]. The results showed that all the Nafion[®]/m-MMT nanocomposite membranes had some moderate thermal stability improvement compared with pristine Nafion[®] and the thermal stability of the composite appeared to be positively correlated with the m-MMT contents as shown in Figure 3.2. The XRD patterns indicated that the side chain groups of Nafion[®] were probably not intercalated into the interlayer of m-MMT; in other hand, the Nafion[®] was probably located outside of the gallery of m-MMT. FT-IR and Si MAS NMR results showed no significant alteration to the lattice structure of m-MMT. The proton conductivities of Nafion[®]/m-MMT nanocomposite membranes were still lower than pure Nafion[®] membrane. The overall proton conductivity decrease for the composite material was moderate (around 4-10%).

In the same year, Mura et al. [4] studied on the proton conductivity of Nafion[®]/Montmorillonite and Nafion[®]/TiO_2 composite membranes by recasting PFSA dispersions. The results showed that the addition of 1 wt% MMT or 1 wt% TiO_2 to the recast membranes did not drastically decrease the conductivity of composite membranes, but increased their water contents. Accordingly, the additives showed a positive effect with respect to the water capacity under dehydration conditions of a proton exchange membrane fuel cell.

Jun et al. [37] prepared Nafion[®]/silicon oxide composite membranes via sol-gel reaction of tetraethylorthosilicate (TEOS) in Nafion[®] membranes, and compared the physical properties with Nafion[®] 1135 membrane. The results in Fig. 3.2 showed that the silicon oxide was compatible with the Nafion[®] membrane and the thermal stability of Nafion[®]/silicon oxide composite membrane was higher than that of Nafion[®] membrane. They found that the silicon oxide of Nafion[®] 1135/silicon oxide composite membrane can absorb water and this part of water mainly existed in the form of structure water and layer water. The tensile strength of Nafion[®]/silicon oxide composite membrane was

almost the same as that of Nafion[®] 1135 membrane. They suggested that the silicon oxide was enhancement function and did not reduce the tensile strength.
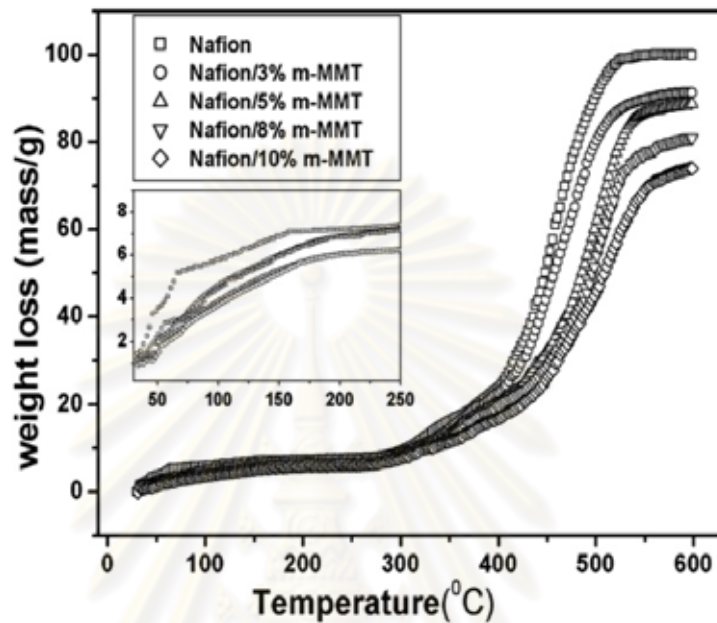
Figure 3.2 Thermal Stability of Nafion[®]/m-MMT with Various Content of m-MMT [11]

CHAPTER IV

EXPERIMENTALS

4.1 Materials

4.1.1 Nafion® perfluorinated resin solution

Nafion® perfluorinated resin solutions with concentration of 5 wt% in lower aliphatic alcohol and water were purchased from Sigma-Aldrich® Co. Density of Nafion® perfluorinated resin solution was 0.874 g/mL at 25 °C and its equivalent weight was 1,100.

4.1.2 Modified Montmorillonite Clay (m-MMT)

Modified Montmorillonite clay used in this study was Bentone SD®-1 as provided by Connell Bros. Co., Ltd., Thailand. The properties of Bentone SD®-1 was shown in Table 4.1.

Table 4.1 Physical properties of Bentone SD®-1
[Bentone SD®-1, Elementis Specialties, Inc.]

Composition	Organic derivative of a bentonite clay
Color/ Form	Very light cream, finely divided powder
Density	1.47 g/cm^3

4.2 Experimental Procedures

4.2.1 Preparation of Composite Membrane

The composite membranes of Nafion® resin with contents of m-MMT at 0, 3, 6, and 10 phr were prepared. The preparation method was based on the works of Kim, Y. et al. [9] and Lin, Y. – F. et al. [10]. The typical steps for preparing Nafion® composite membranes at 3 phr m-MMT were the following. The 0.187 grams of modified-

Montmorillonite (m-MMT) clay was added into 142.72 ml of 5 wt% Nafion® perfluorinated resin solution, then stirred mechanically for 3 h and degassed by ultrasonication for 2 h. The prepared mixture was then poured into 15-cm diameter Petri dish and dried in vacuum oven by slowly increasing the temperature from room temperature to 85 °C within 3.5 h to prevent the crevice to form in the composite membrane and held at 85 °C for another 20.5 h. Finally, the composite membrane was pre-treated in a standard manner: boiled in 5% H_2O_2 solution at 80 °C for 1 h, boiled in 1 M H_2SO_4 solution at 80 °C for at least 2 h, and boiled in deionized water at 80 °C for 1 h. The thickness of final membrane was expected to be around 0.0178 cm or 0.007 in. The total weight was around 6.424 g. and the weight of Nafion® in the membrane was 6.237 g.

The calculation of the actual amount of m-MMT for making Nafion®/m-MMT composite membrane at 3, 6, and 10 phr were shown in Appendix A.

4.2.2 Characterization

4.2.2.1 X-Ray Diffraction (XRD)

Inter-layer spacing between clay platelets of m-MMT in the membranes were measured by X-ray diffraction (XRD) method with Bruker AXS Model D8 Discover (as shown in Figure 4.1) with CuK radiation. The machine was located at the Scientific and Technological Research Equipment Centre, Chulalongkorn University. The voltage and the current of X-ray beams were 40 kV and 40 mA, respectively. XRD data were collected between 1 and 20° by a step of 0.025° with a scan speed of 1 second/step.

4.2.2.2 Ion Exchange Capacity (IEC)

IEC (mmol of proton per dry weight of membrane) was measured by titration method. The dried acid-form membranes were weighed and then soaked in 1 M NaCl solution for 24 h to fully exchange sodium ions for the protons in the membranes. The exchanged protons which contained in NaCl solution were titrated with 0.0125 M NaOH solution using phenolphthalein as indicator. The titrations were repeated 3 times and the average IEC was reported. The IEC was calculated by the following equation,

$$IEC = \frac{C_{NaOH}V_{NaOH}}{W_{dry}} \qquad (4.1)$$

where C_{NaOH} and V_{NaOH} are molar concentration and titration volume of NaOH solution, respectively, and W_{dry} is dry weight of membrane.
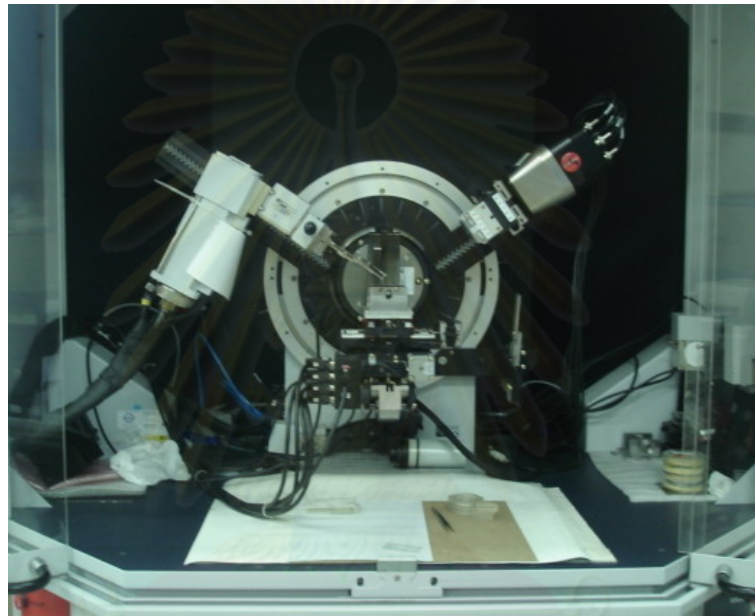
Figure 4.1 X-Ray Diffraction Spectrometer

4.2.2.3 Water Uptake

The composite membranes were dried in vacuum oven at 100 °C for 24 h and weighed. The membranes were then immersed in deionized water for 24 h and weighed. The water uptake of membranes was calculated using the following equation,

$$WaterUptake = \frac{W_{wet} - W_{dry}}{W_{dry}} \times 100\% \qquad (4.2)$$

where W_{dry} and W_{wet} are weight of membranes in dried and soaked conditions, respectively.

4.2.2.4 Tensile Properties Measurement

The Nafion[®] membranes and Nafion[®]/m-MMT composite membranes were cut into the rectangular specimens (1 cm x 10 cm), as shown in section 2.6.3, Figure 2.17, according to ASTM D882 for tensile properties measurement of thin plastic sheeting. The prepared test specimens were tested by Universal Testing Machine (Instron[®] Instrument, Model 5567), as shown in Figure 4.2, with the initial distance between grips of 5 cm and the rate of grips separation of 5 mm/min. The 1 kN load cell was used.

4.2.2.5 Determination of Thermal Properties

Thermal properties of Nafion[®]/m-MMT composite membranes were tested by Differential Scanning Calorimeter (DSC), TA Instruments 2910, as shown in Figure 4.3. The samples were cut into small pieces and weighed in range of 5 - 10 mg and then placed in aluminum pan. The sample pan and reference pan were placed in the furnace and burned under nitrogen condition in the temperature range of 25 – 300 °C with scanning rate of 10 °C/min.

Figure 4.2 Universal Testing Machine

Figure 4.3 Differential Scanning Calorimeter (DSC)

CHAPTER V

RESULTS AND DISCUSSIONS

The pristine Nafion[®] membrane and Nafion[®]/m-MMT composite membranes prepared in this study had the uniform thickness ca. 0.0178 cm. The pictures of all membranes were shown in Figure 5.1.
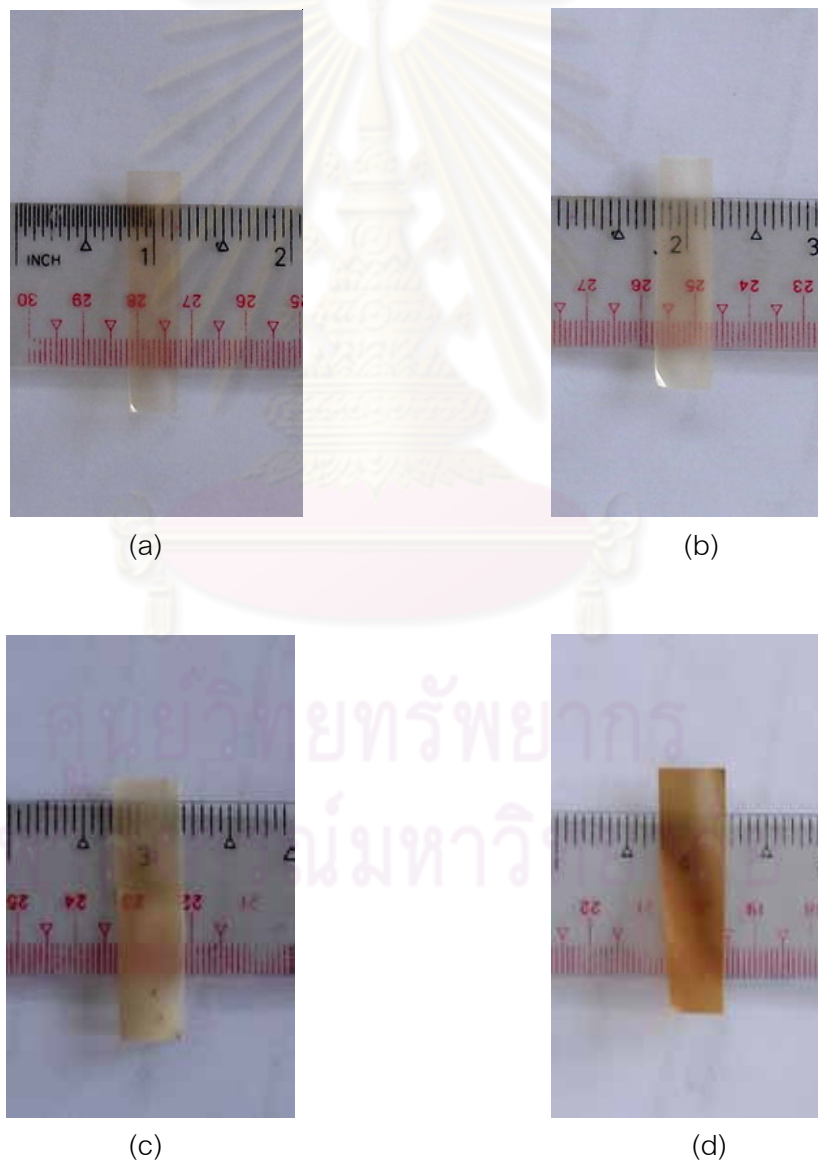
Figure 5.1 Pictures of (a) Pristine Nafion[®] Membrane and
Nafion[®]/m-MMT Composite Membranes at (b) 3 phr, (c) 6 phr, and (d) 10 phr

From Figure 5.1, the pristine Nafion[®] was a translucent film but all the composite membranes were not as clear because of m-MMT in the films. The composite membranes were more brownish with increasing amount of m-MMT in Nafion[®] membrane. The composite membranes were clearer after boiled in H_2O_2.

5.1 X-Ray Diffraction Patterns of Nafion[®] and Nafion[®]/m-MMT Composite Membranes

The XRD patterns of pristine Nafion[®] membrane, modified Montmorillonite (m-MMT) clay and Nafion[®]/m-MMT composite membranes with various contents of m-MMT were determined as described in Chapter IV. The XRD patterns were shown in Figure 5.2. The calculation of interlayer spacing between clay platelets according to the Bragg's law ($2d \sin\theta = \lambda$) was shown in Appendix B, and the results were shown in Table 5.1.

From Figure 5.2, the pristine Nafion[®] membrane showed no distinct peak. The m-MMT showed the diffraction peak at $2\theta = 2.38°$, hence, the interlayer spacing of m-MMT was 3.71 nm. This result was consistent with result obtained by Pirotesak [21]. The Nafion[®]/m-MMT composite membranes with the contents of m-MMT of 3, 6, and 10 phr showed the diffraction peaks at $2\theta = 6.30°$, $6.45°$, and $6.31°$, respectively. These peaks were clearly from the m-MMT added into Nafion[®] matrix. The interlayer spacing of m-MMT in these composite membranes were 1.40, 1.37, and 1.40 nm, respectively. These results indicated that the interlayer spacing of m-MMT was decreased when incorporated into Nafion[®] matrix.

It should be noted that the diffraction peaks of m-MMT in the Nafion[®]/m-MMT composite membranes occurred nearly in the same position (approximately $2\theta = 6.35°$). The average d-spacing of interlayer of m-MMT in the composite membranes was 1.39 nm. According to the previous studies, the d-spacing of unmodified MMT clay was around 1.24 - 1.39 nm [9, 10]. This d-spacing was very close to the d-spacing of m-MMT in the Nafion[®]/m-MMT composite membranes obtained in this work. Hence, the decrease in d-spacing of m-MMT in the composite membranes prepared in this work may be due to partial leaching out of the modified functional

groups of m-MMT during membrane preparation steps. This average d-spacing of 1.39 nm also suggested that the Nafion[®] matrix did not intercalate into the interlayer spacing of m-MMT clay. Therefore, the prepared Nafion[®]/m-MMT composite membranes should be of the conventional composite type.

Table 5.1 The Interlayer Spacing of m-MMT Clay and of m-MMT clay in the
Nafion[®]/m-MMT Composite Membranes

Samples	2-theta (°)	d-spacing (nm)
m-MMT	2.38	3.71
Nafion[®]/3 phr m-MMT	6.30	1.40
Nafion[®]/6 phr m-MMT	6.45	1.37
Nafion[®]/10 phr m-MMT	6.31	1.40
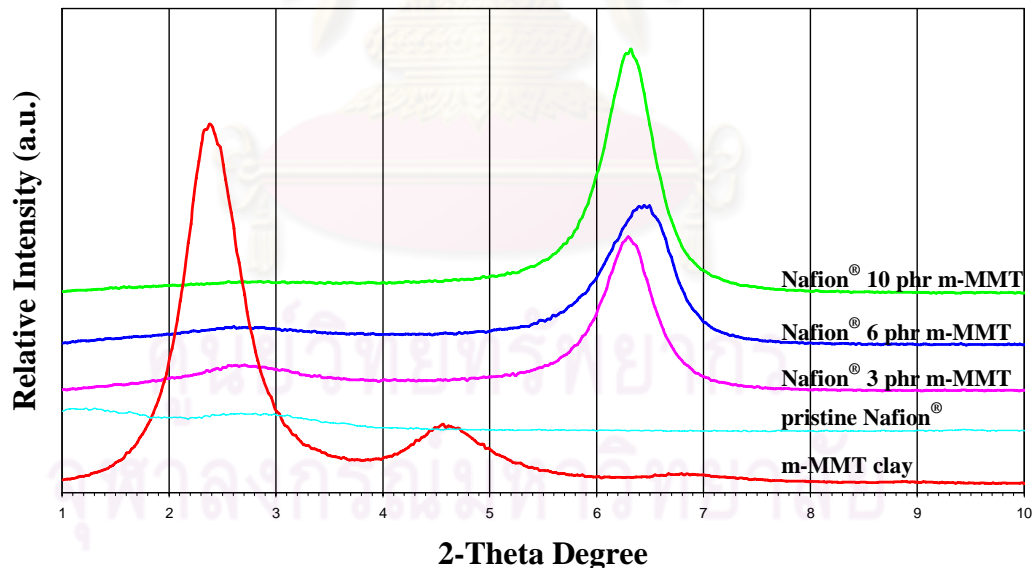
Figure 5.2 XRD Patterns of m-MMT, Pristine Nafion[®] Membrane and Nafion[®]/m-MMT Composite Membranes containing m-MMT at 3 phr, 6 phr, and 10 phr.

5.2 Water Uptake and Ion Exchange Capacity (IEC)

The water uptake and IEC of pristine Nafion[®] membrane and Nafion[®]/m-MMT composite membranes were measured by the procedures described in Chapter IV. The values of the water uptake and IEC were shown in Table 5.2.

Table 5.2 Water Uptake and IEC Values of Pristine Nafion[®] and Nafion[®]/m-MMT Composite Membranes

Samples	Water Uptake at room condition (%)	Water Uptake at 100 °C (%)	IEC (mmol/g membrane)	IEC (mmol/g Nafion[®])
pristine Nafion[®]	20.31	46.63	0.89	0.89
Nafion[®]/3 phr m-MMT	25.62	62.33	0.79	0.82
Nafion[®]/6 phr m-MMT	26.02	60.43	0.76	0.81
Nafion[®]/10 phr m-MMT	27.73	48.78	0.73	0.81

From Table 5.2, the water uptake after 24 h at room temperature of the composite membranes was increased with increasing contents of m-MMT in the Nafion[®] matrix. For example, the water uptake of pristine Nafion[®] was 20.31% and Nafion[®]/m-MMT (10 phr) composite membrane was 27.73%. The Nafion[®]/m-MMT (10 phr) composite membrane showed an increase of 36.53% from the pristine Nafion[®] membrane. This increase in water uptake should be due to the water uptake of m-MMT. Although, m-MMT was hydrophobic filler but the m-MMT in Nafion[®] matrix in this study was more of hydrophilic type because the modified function on m-MMT surface was likely to be partially leached out during membrane preparation (as noted in section 5.1 above).

After submerged in water at 100 °C for 1 h, the water uptake of the composite membranes also generally increased with increasing contents of m-MMT in the Nafion® matrix. For example, the water uptake of pristine Nafion® was 46.63% and Nafion®/m-MMT (6 phr) composite membrane was 60.43%. It should be noted that the water uptake of Nafion®/m-MMT (10 phr) composite membrane was only 48.78%. This might be an error due to poor choice of sample used.

When the water uptakes of all membranes at room temperature were compared with the values at 100 °C, it could be seen that in general the water uptakes at 100 °C were about 2 times of the values at room temperature. This result was consistent with the work of Satterfield et al. [34] who also suggested that the water sorption of Nation®-type membrane might be controlled by kinetics and water sorption was not in thermodynamic equilibrium at room temperature within 24 h.

Also from Table 5.2, the Ion Exchange Capacities (IECs) of composite membranes were slightly decreased with increasing amount of m-MMT. For example, the IEC of pristine Nafion® was 0.89 mmol/g membrane and Nafion®/m-MMT (10 phr) composite membrane was 0.73 mmol/g membrane. The IEC of 10 phr composite membrane showed a decrease of 17.98% from the pristine Nafion® membrane. This decrease in IEC was conformed to the previous study of Lin et al. [10]. This decrease could be due to lower amount of Nafion® in the composite membrane than in the pristine Nafion® membrane when compared at equal total weight. When compared IEC values of the membranes by gram of Nafion®, the results showed that the IEC values of 3 types of composite membranes were closely equal (around 0.81 mmol/g Nafion®) but still lower than that of the pristine Nafion® membrane (at 0.89 mmol/g Nafion®). It was suggested that there were no counter ions located between the interlayer spacing of m-MMT clay [10].

The transfer of protons in Nafion® membrane depends on water content of the membrane and there are various proton transport mechanisms as suggested in Figure 2.9 [17]. Although the IEC values of Nafion®/m-MMT composite membranes prepared in this work decreased with increasing amount of m-MMT but the water uptake of

Nafion®/m-MMT composite membrane increased with increasing amount of m-MMT. Hence, as the membrane becomes more saturated, it may give rise to the bulk-like portion of water leading to bulk-like transfer that gives high rate of proton transfer in the middle of pores [17]. Therefore, it was speculated in this work that the effects of higher water uptake and lower IEC values on proton transfer of the Nafion®/m-MMT composite membranes prepared in this work would balance each other out and, hence, the proton conductivity of Nafion®/m-MMT composite membranes prepared in this work would not differ from the pristine Nafion® membrane.

5.3 Effect on Thermal Properties of Nafion® Membrane and Nafion®/m-MMT Composite Membranes

The DSC scanning results for the samples were shown in Figure 5.3. All the samples were placed in room condition before scanning.
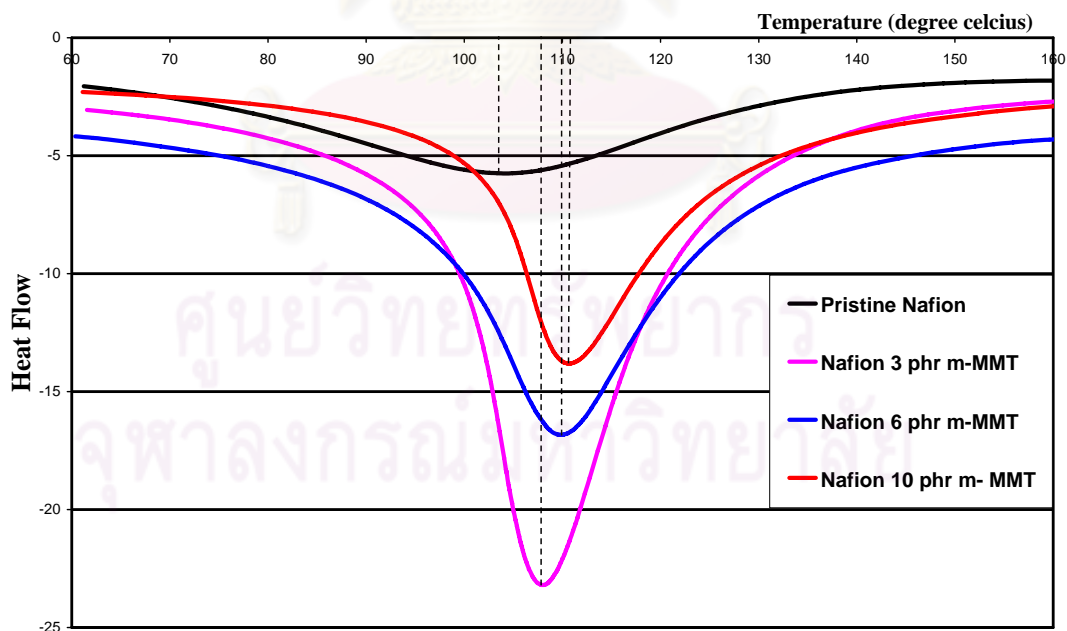
Figure 5.3 DSC Curves of Nafion® Membrane and
Nafion®/m-MMT Composite Membranes

It was observed that the Nafion[®] membrane showed a peak at 103 °C, while the peaks of Nafion[®]/m-MMT composite membranes were at higher temperature. From Figure 5.3, the peaks of the composite membranes increased with increasing amount of m-MMT. From the previous study, Corti et al. [35] implied that the peak in the range of 100 – 150 °C corresponds to the desorption of the water from the membrane. Hence, it could be said that the higher peak suggested that the water in the membrane was harder to remove from the composite membrane. In another words, the water retention of Nafion[®] membrane was improved by incorporating m-MMT into Nafion[®] matrix to fabricate the composite membrane.

5.4 Effects on Mechanical Properties of Nafion[®] Membrane and Nafion[®]/m-MMT Composite Membranes

According to ASTM D882, the specimens of Nafion[®] membrane and Nafion[®]/m-MMT composite membranes were prepared as described in Chapter IV. The elastic modulus and elongation at break data were summarized in Table 5.3 and in Figure 5.4 and Figure 5.5, respectively. The hydrated specimens were soaked in deionized water for 24 h before tested. All the samples were also tested at room temperature.

From Table 5.3 and Figure 5.4, the elastic modulus of soaked Nafion[®] membrane was remarkably different from Nafion[®] membrane at room condition. The elastic modulus of Nafion[®] membrane was decreased from 198.16 MPa to 121.22 MPa when Nafion[®] membrane was fully hydrated. This was a decrease of about 38.83%. This result was in the same direction of Satterfield et al. [34]. This suggested that water absorption reduced the elastic modulus of Nafion[®] membrane by acting as a plasticizer.

When the moduli of fully hydrated Nafion[®] membrane and Nafion[®]/m-MMT composite membranes were compared, the results in Table 5.3 showed that the elastic modulus of all types of the composite membranes were not much different from the pristine Nafion[®] membrane. The elastic moduli of all soaked membranes were on average around 118-120 MPa as can be seen in Figure 5.4. It was also noted that the elastic modulus of the soaked Nafion[®]/m-MMT composite membranes did not

decreased with increasing amount of m-MMT. Although the water uptake of Nafion[®]/m-MMT composite membranes increased with increasing m-MMT as shown in Table 5.2 and it might be expected that the elastic modulus of Nafion[®]/m-MMT composite membranes should decrease with increasing water content as water acted as plasticizer [34], the result in this work showed that the incorporation of m-MMT in composite can at least helped reduce the decay of the mechanical property of the Nafion[®]/m-MMT composite membranes. Hence, the m-MMT can act as reinforcing filler in the composite.

Table 5.3 Mechanical Properties of Pristine Nafion[®] and
Nafion[®]/m-MMT Composite Membranes

Samples	Elastic Modulus (MPa)	Elongation at Break (%)
Pristine Nafion[®] (room condition)	198.16 $\pm$ 35.05	277.40 $\pm$ 27.97
Pristine Nafion[®] (soaked)	121.22 $\pm$ 14.52	185.00 $\pm$ 51.34
Nafion[®]/3 phr m-MMT (soaked)	119.42 $\pm$ 12.14	58.60 $\pm$ 33.80
Nafion[®]/6 phr m-MMT (soaked)	111.58 $\pm$ 9.63	114.80 $\pm$ 26.50
Nafion[®]/10 phr m-MMT (soaked)	122.91 $\pm$ 35.05	71.00 $\pm$ 5.83
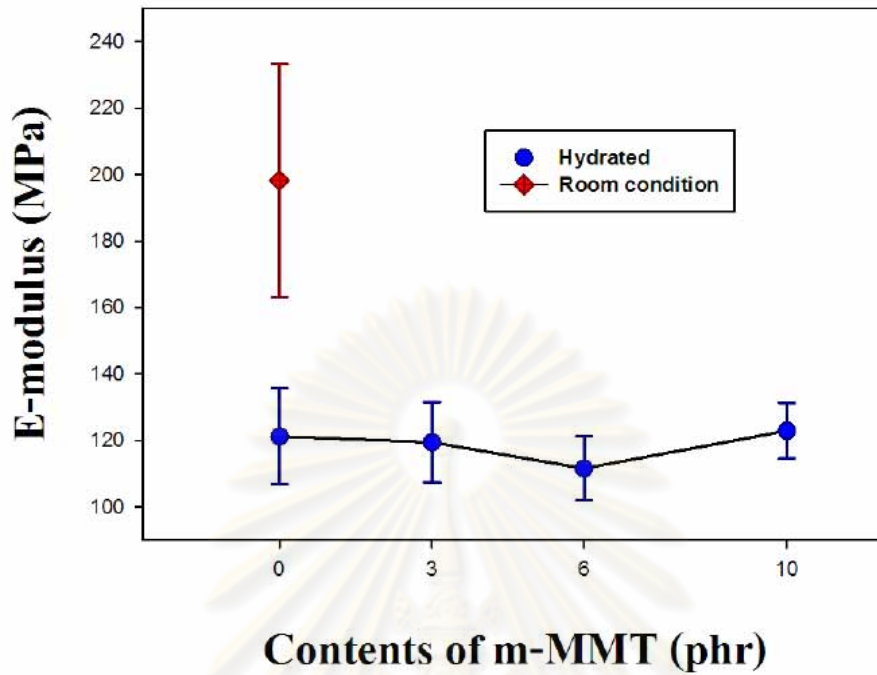
Figure 5.4 Elastic Modulus of Nafion[®]/m-MMT Composite Membranes
with Various Contents of m-MMT
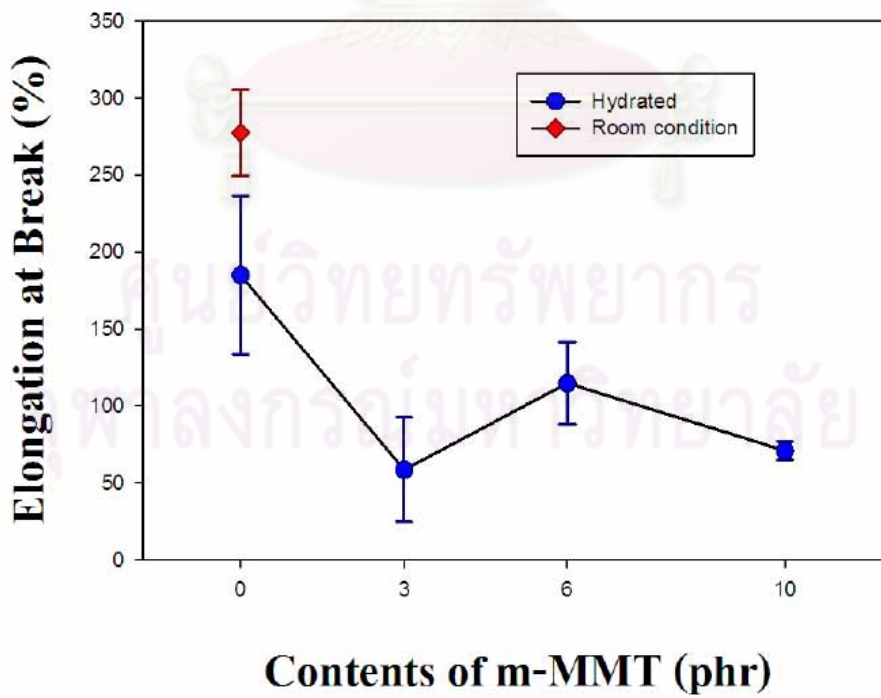
Figure 5.5 Elongation at Break of Nafion[®]/m-MMT Composite Membranes
with Various Contents of m-MMT

Regarding the elongation at break of the membranes (Table 5.3 and Figure 5.5), the pristine Nafion[®] membrane that was placed at room condition had higher percent elongation at break (277.40%) than that of soaked pristine Nafion[®] membrane (185.0%). That was a 33.31% reduction.

The elongation at break of soaked Nafion[®]/m-MMT composite membranes were significantly decreased by addition of m-MMT into Nafion[®] membranes but the effect of m-MMT content was not clear. The elongation at break of soaked composite membranes was reduced from 185.0% of pristine Nafion[®] membrane to around 81.50% on average for soaked Nafion[®]/m-MMT composite membranes with m-MMT contents in range of 3-10 phr. From this result, it can be concluded that the Nafion[®]/m-MMT composite membranes prepared in this work were more brittle than the pristine Nafion[®] membrane.

According to the results in section 5.1, the Nafion[®] membrane did not intercalate into the interlayer spacing of m-MMT and the composite membranes were expected to be of conventional type. And as the content of m-MMT in composites was low (up to 10 phr only), hence, there should not be much improvement effect of m-MMT on mechanical properties of the composite membranes.

The content of water in the membrane showed significant effect on the mechanical properties of the membrane. The Nafion[®] membrane became more flexible after absorption of water, as shown in Table 5.3. From the literature reviews [17, 34], it could be predicted that the elastic modulus and elongation at break of the composite membranes would be decreased when the composite membranes were hydrated. Moreover, the mechanical properties of Nafion[®] membrane depended on temperature [17, 34]. The elastic modulus of the membrane was also decreased with increasing temperature.

According to the chemical structure of Nafion[®] membrane, the polytetrafluoroethylene (PTFE) backbone is an extreme hydrophobic domain and the terminal sulfonated groups are extreme hydrophilic domain. In the presence of water, the sulfonated groups are hydrated to maintain the proton conductivity, while the

polytetrafluoroethylene (PTFE) backbone provides mechanical strength. In addition, high proton conductivity can be obtained at high sulfonate groups, but high sulfonate groups results in high water uptake.

It was concluded in this work that the elastic moduli of soaked Nafion[®]/m-MMT composite membranes were about equal to the soaked pristine Nafion[®] membrane, and the elongation at break of the soaked Nafion[®]/m-MMT composite membranes were lower than that of soaked pristine Nafion[®] membrane. Therefore, the incorporation of this m-MMT clay type (Bentone SD[®] 1) into Nafion[®] matrix did not improve the mechanical properties of Nafion[®] membrane but at least helped reduce the decay of the these mechanical properties by counteracting the effects of increasing water uptake in the composite membranes.

CHAPTER VI

CONCLUSIONS & RECOMMENDATIONS

6.1 Conclusions

From the results obtained in this work, the following conclusions can be made.

1. The typical properties of pristine Nafion® membrane prepared in this work by solution mixing method was conformed to that of the commercial Nafion® membrane.

2. The XRD patterns showed the decrease of interlayer spacing of m-MMT clay after incorporated into Nafion® matrix. This decrease might be due to partial leach out of the modified function of m-MMT clay during membrane preparation. The d-spacing reduction also indicated that Nafion®/m-MMT composite membranes prepared in this work were of the conventional composite.

3. The water uptake of Nafion®/m-MMT composite membrane increased with increasing amount of m-MMT clay in Nafion® matrix but the IEC values of Nafion®/m-MMT composite membranes decreased. These effects would balance each other out and, hence, the proton conductivity of Nafion®/m-MMT composite membranes prepared in this work would not differ from the pristine Nafion® membrane.

4. Nafion®/m-MMT composite membranes could retain water better than pristine Nafion® membrane at high temperature.

5. The elastic moduli of soaked Nafion®/m-MMT composite membranes were about equal to the soaked pristine Nafion® membrane, and the elongation at break of the soaked Nafion®/m-MMT composite membranes were lower than that of soaked pristine Nafion® membrane. Therefore, the incorporation of this m-MMT clay type (Bentone SD® 1) into Nafion® matrix did not improve the mechanical properties of Nafion® membrane but at least helped reduce the decay of the these mechanical properties by counteracting the effects of increasing water uptake in the composite membranes.

6.2 Recommendations

To further the understanding the usefulness of Nafion$^®$/m-MMT composite membranes, the following recommendations were made.

1. To obtain intercalated or exfoliated nanocomposite, the filler should be more compatible with the polymer and should have more tightly bond between the modified function and clay platelet, hence, new kind of filler should be studied.

2. The Nafion$^®$ membrane and Nafion$^®$/m-MMT composite membranes should be tested by Thermal Gravimetric Analyzer (TGA) to obtain more information on the thermal stability of the membranes.

3. To observe the dispersion of modified-Montmorillonite clay in the Nafion$^®$ matrix and to gain more understanding on the morphology of the composite membranes, the Scanning Electron Microscope (SEM) should be used to study the composite membranes.

4. All membranes should be tested for the methanol permeability to study their applicability as membrane for the Direct Methanol Fuel Cell.

5. All membranes should be tested for proton conductivity to study their applicability as membrane for fuel cell.

REFERENCES

[1]   Godwin, M., and Gardner, S. Global warming[online]. California, USA:
        Wikipedia, the free encyclopedia (Distributor), (n.d.). Available from:
        http://en.wikipedia.org/wiki/Global_warming

[2]   Godwin, M., and Gardner, S. Clean energy trends[online]. California, USA:
        Wikipedia, the free encyclopedia (Distributor), (n.d.). Available from:
        http://en.wikipedia.org/wiki/Clean_Energy_Trends

[3]   Godwin, M., and Gardner, S. fuel cell [online]. California, USA: Wikipedia,
        the free encyclopedia (Distributor), (n.d.). Available from:
        http://en.wikipedia.org/wiki/fuel_cell

[4]   Mura, F.; Silva, R. F.; and Pozio, A. Study on the conductivity of recast
        Nafion®/montmorillonite and Nafion®/TiO$_2$ composite membranes.
        Electrochimica Acta 52 (March 2007): 5824-5828.

[5]   Thomassin, J.-M.; Pagnoulle, C.; Caldarella, G.; Germain, A.; and Jerome, R.
        Impact of acid containing montmorillonite on the properties of Nafion®
        membranes. Polymer 46 (October 2005): 11389-11395.

[6]   Sacca, A.; Carbone, A.; Pedicini, R.; Portale, G.; D'Ilario, L.; Longo, A.;
        Martorana A.; and Passalaequa, E. Structure and electrochemical
        investigation on re-cast Nafion membranes for polymer electrolyte   fuel
        cells (PEFCs) application. Journal of Membrane Science 278 (2006):
        105-113.

[7]   Rhee, C. H.; Kim, Y.; Lee, J. S.; Kim, H. K.; and Chang, H. Nanocomposite
        membranes of surface-sulfonated titanate and Nafion® for direct
        methanol fuel cells. Journal of Power Sources 159 (January 2006): 1015-
        1024.

[8]   Thomassin, J.-M.; Pagnoulle, C.; Bizzari, D.;   Caldarella, G.; Germain, A.; and Jerome, R.   Improvement of the barrier properties of Nafion[®] by fluoro-modified montmorillonite. Solid State Ionics 177 (April 2006): 1137-1144.

[9]   Kim, Y.; Lee, J. S.; Rhee, C. H.; Kim, H. K.; and Chang, H. Montmorillonite functionalized with perfluorinated sulfonic acid for proton-conducting organic-inorganic composite membranes.   Journal of Power Sources 162 (September 2006): 180-185.

[10]   Lin, Y.-F.; Yen, C.-Y.; Ma, C.-C. M.; Liao, S.-H.; Hung, C.H.; and Hsiao, Y.H. Preparation and properties of high performance nanocomposite proton exchange membrane for fuel cell.   Journal of Power Sources 165 (January 2007): 692-700.

[11]   Zhang, L.; Xu, J.; Hou, G.; Tang, H.; and Deng, F. Interactions between Nafion resin and protonated dodecylamine modified montmorillonite: A solid state NMR study. Journal of colloid and Interface Science 311 (February 2007): 38-44.

[12]   Zhang, J.; Xie, Z.; Zhang, J.; Tang, Y.; Song, C.; Navessin, T.; Shi, Z.; Song, D.; Wang, H.; Wilkinson, D. P.; Liu, Z.-S.; and Holdcroft, S.   High temperature PEM fuel cells: Review. Journal of Power Sources   160 (June 2006): 872-891.

[13]   Ramani, V. Fuel Cells. The electrochemical Society Interface (2006): 41-44.

[14]   Schilling, H.   Fuel cell [Online]. USA: NASA, (n.d.). Available from: http://www.grc.nasa.gov/www/electrochemistry/images/fuel_cell.jpg

[15]   Types of fuel cells [Online]. USA: U.S. Department of Energy's office of Energy Efficiency and Renewable Energy, (n.d.). Available from: http://www1.eere.energy.gov/hydrogenandfuelcells/fuelcells/fc_types.html

[16]   Types of fuel cells [Online]. USA: Rocky Mountain Institute, (n.d.). Available from: http://www.rmi.org/sitepages/pid556.php

[17]   Jalani,   N.   H.   Development   of   Nanocomposite   Polymer   Electrolyte
       Membranes   for   Higher   Temperature   PEM   Fuel   cells.   Doctoral
       dissertation, Chemical Engineering, Faculty of Worchester Polytechnic
       Institute. 2006.

[18]   Fuel   cells   [Online].   Italy: Micro-Vett   SPA.,   (n.d.).   Available   from:
       http://www.micro-vett.it/h2/ing/fcing.html

[19]   Hickner, M. A.; Ghassemi, H.; Kim, Y. S.; Einsla, B. R.; and McGrath, J. E.
       Alternative Polymer Systems for Proton Exchange Membranes (PEMs).
       Chemical Reviews 104 (2004): 4587-4612.

[20]   Grim, R. E. Clay mineralogy. 2nd ed. New York: McGraw-Hill, 1968.

[21]   Nuchjaree Pirotesak.   Analysis of Young's Modulus of Polypropylene/clay
       nanocomposite.   Master's Thesis, Department of Chemical Engineering,
       Faculty of Engineering, Chulalongkorn University. 2006.

[22]   Piyaporn Kampeerapappun.   Preparation of cassava starch/montmoillonite
       nanocomposite film.   Master's Thesis, Faculty of Science, Chulalongkorn
       University. 2003.

[23]   Barthelmy,   D.   Montmorillonite   [Online].   Australia: (n.d.).   Available   from:
       http://webmineral.com/specimens/picshow.php?id=1285

[24]   Ray, S. S., and Okamoto, M. Polymer/layered silicate nanocomposites: a
       review from preparation to processing. Progress in Polymer Science 28
       (2003): 1539-1641

[25]   Wenk, H.-R. and Bulakh, A. Minerals: Their Constitution and origin. England:
       Cambridge University Press, 2004.

[26]   Unique   NRC-Industry   Research   Partnership   Lunched[Online].   Canada:
       National   Research   Council   of   Canada,   2003.   Available   from:
       http://www.nrc-cnrc.gc.ca/highlights/2003/0307nanocomp_e.html

[27]   Askeland, D. R. and Phule, P. P.   Essentials of materials science and
       engineering. Australia: Thompson, 2004.

[28]   Budinski, K. G. and Bundinski, M. K. Engineering materials: properties and selection. 8th ed. Upper Saddle River, N.J.: Pearson Prentice Hall, 2005.

[29]   Tensile Properties [Online]. USA: (n.d.). Available from: http://www.ndt-ed.org/EducationResources/CommunityCollege/Materials/Mechanical/Tensile.htm

[30]   Koo, J. H. Polymer nanocomposite: processing, characterization, and applications. McGraw-Hill nanoscience and technology series. New York: McGraw-Hill, 2006.

[31]   Richard, G. A. Bragg's law and diffraction: How waves reveal the atomic structure of crystals [Online]. New York, USA: Schields, P. J., 2003. Available from: http://www.mpi.stonybrook.edu/SummerScholars/2003/ Projects/RGonzalez/BraggsLawApplet/index.html

[32]   Carraher, Jr. C. E. Polymer Chemistry. 6th ed. revised and expanded. USA: Marcel Dekker, 2003.

[33]   Differential scanning calorimetry [Online]. Australia: Rapid Intelligence, (n.d.). Available from: http://www.nationmaster.com/encyclopedia/ Differential-scanning-calorimetry

[34]   Satterfield, M. B.; Majsztrik, P. W.; Ota, H.; BenZiger, J. B.; and Bocarsly, A. B. Mechanical properties of Nafion and titania/Nafion composite membranes for polymer electrolyte membrane fuel cells. Journal of Polymer Science 44 (April 2006): 2327-2345.

[35]   Corti, H. R.; Nores-Pondal, F.; and Buera, M. P. Low temperature thermal properties of Nafion 117 membranes in water and   methanol-water mixtures. Journal of Power Sources (June 2006)

[36]   Kim, T. K.; Kang, M.; Choi, Y. S.; Kim, H. K.; Lee, W.; Chang, H.; and Seung, D. Preparation of Nafion-sulfonated clay nanocomposite membrane for direct methanol fuel cells via a film coating process. Journal of Power Source 165 (November 2007): 1-8.

[37]   Jun,Y.; Mu, P.; and Runzhang, Y. Nafion/silicon oxide composite membrane for high temperature proton exchange membrane fuel cell. <u>Journal of Wuhan University of Technology-Mater</u> 22 (September 2007): 47

APPENDICES

Appendix A

The Calculation of m-MMT amount

The volume of membrane with thickness of 7 mil or 0.0178 cm that cast in the Petri dish with diameter of 15 cm was calculated by

$$\pi\left(\frac{15}{2}\right)^2 (0.0178) = 3.15 \ cm^3$$

The density of Nafion® membrane $\qquad = \ 1.98 \ \dfrac{g}{cm^3}$

Then the weight of Nafion® membrane $\qquad = \ \left(3.15 \ cm^3\right)\left(\dfrac{1.98 \ g}{cm^3}\right)$

$$= \ 6.237 \ g$$

The desired volume (V) of Nafion® resin solution (5 wt% in lower aliphatic alcohol and water) with density of $0.874 \ \dfrac{g}{cm^3}$ was calculated by

$$\left(\frac{5}{100}\right)\left(0.874 \ \frac{g}{cm^3}\right)V \ = \ 6.237 \ g$$

$$V \ = \ 142.72 \ ml$$

From the weight of Nafion® resin (6.237 g), the amount of m-MMT clay, which was mixed into Nafion® solution, was shown in Table A-1.

Table A-1 Amount of Modified-Montmorillonite Clay in the Composite Membrane

Part per Hundred Resin	Weight of Nafion® resin (g)	Weight of m-MMT Clay (g)
3 phr	6.237	0.187
6 phr	6.237	0.374
10 phr	6.237	0.624

Appendix B

D-spacing Calculation

The d-spacing of organo-clay in the polymer composite was calculated by Bragg's law equation as shown below,

$$2d \sin \theta = n\lambda$$

where d is the spacing between atomic planes in the crystalline phase

λ is the x-ray wavelength

θ is the reflection angle

n is the order of reflection

Diffraction angle of organo-clay powder was measured by XRD. The peak was at $2\theta = 2.38°$, hence, the d-spacing of organo-clay powder was

$$(2)d \sin(2.38/2) = (1)(1.542)$$
$$d = 1.542/2/\sin 1.19$$
$$d = 3.71 \, nm$$

Appendix C

Water Uptake and IEC

Table C-1 Raw Data for Water Uptake at Room Temperature of Pristine Nafion[®]

Membrane and Nafion[®]/m-MMT Composite Membranes

pristine Nafion[®]	Specimen	Dry weight (g)	Wet weight (g)	% water uptake
	1	0.41	0.55	32.64
	2	0.45	0.49	8.60
	3	0.50	0.60	20.21
	4	0.53	0.64	20.17
	5	0.53	0.63	19.96
	Mean			20.31
	S.D.			8.50
Nafion[®]/3 phr m-MMT	Specimen	Dry weight (g)	Wet weight (g)	% water uptake
	1	0.50	0.62	25.30
	2	0.49	0.61	26.08
	3	0.49	0.62	26.50
	4	0.46	0.57	25.32
	5	0.45	0.56	24.90
	Mean			25.62
	S.D.			0.65
Nafion[®]/6 phr m-MMT	Specimen	Dry weight (g)	Wet weight (g)	% water uptake
	1	0.49	0.62	25.91
	2	0.46	0.58	26.02
	3	0.49	0.61	25.73
	4	0.50	0.63	25.91
	5	0.50	0.63	26.52
	Mean			26.02
	S.D.			0.30
Nafion[®]/10 phr m-MMT	Specimen	Dry weight (g)	Wet weight (g)	% water uptake
	1	0.44	0.56	27.12
	2	0.47	0.60	27.79
	3	0.49	0.62	26.54
	4	0.50	0.63	26.93
	5	0.51	0.66	30.25
	Mean			27.73
	S.D.			1.48

Table C-2 Raw Data for Water Uptake of Pristine Nafion[®] Membrane and Nafion[®]/m-MMT Composite Membranes Boiled in Water at 100 °C for 1 hr

pristine Nafion[®]	Specimen	Dry weight (g)	Wet weight (g)	% water uptake
	1	0.126	0.184	46.03
	2	0.104	0.154	48.08
	3	0.083	0.121	45.78
	Mean			46.63
	S.D.			1.26
Nafion[®]/3 phr m-MMT	Specimen	Dry weight (g)	Wet weight (g)	% water uptake
	1	0.292	0.478	63.70
	2	0.205	0.331	61.46
	3	0.186	0.301	61.83
	Mean			62.33
	S.D.			0.91
Nafion[®]/6 phr m-MMT	Specimen	Dry weight (g)	Wet weight (g)	% water uptake
	1	0.261	0.424	62.45
	2	0.230	0.369	60.43
	3	0.262	0.415	58.40
	Mean			60.43
	S.D.			1.35
Nafion[®]/10 phr m-MMT	Specimen	Dry weight (g)	Wet weight (g)	% water uptake
	1	0.282	0.413	46.45
	2	0.166	0.247	48.80
	3	0.231	0.349	51.08
	Mean			48.78
	S.D.			1.55

Table C-3 Raw Data for IEC Values of Pristine Nafion[®] Membrane and Nafion[®]/m-MMT

Composite Membranes

pristine Nafion[®]	Specimen	Dry Weight (g)	NaOH 0.05M (ml)	H$^+$ (mmol)	IEC (mmol/g membrane)	IEC (mmol/g Nafion[®])
	1	0.2211	4.0000	0.2000	0.9046	
	2	0.1268	2.2000	0.1100	0.8675	
	3	0.1687	3.0000	0.1500	0.8892	
	Mean				0.8871	
	S.D.				0.0186	
Nafion[®]/ 3 phr m-MMT	Specimen	Dry Weight (g)	NaOH 0.025M (ml)	H$^+$ (mmol)	IEC (mmol/g membrane)	IEC (mmol/g Nafion[®])
	1	0.1359	4.4000	0.1100	0.8094	0.8345
	2	0.1346	4.2000	0.1050	0.7801	0.8042
	3	0.1082	3.4000	0.0850	0.7856	0.8099
	Mean				0.7917	0.8162
	S.D.				0.0156	0.0161
Nafion[®]/ 6 phr m-MMT	Specimen	Dry Weight (g)	NaOH 0.025M (ml)	H$^+$ (mmol)	IEC (mmol/g membrane)	IEC (mmol/g Nafion[®])
	1	0.1171	3.7000	0.0925	0.7899	0.8403
	2	0.1265	3.9000	0.0975	0.7708	0.8199
	3	0.1023	3.0000	0.0750	0.7331	0.7799
	Mean				0.7646	0.8134
	S.D.				0.0289	0.0307
Nafion[®]/ 10 phr m-MMT	Specimen	Dry Weight (g)	NaOH 0.025M (ml)	H$^+$ (mmol)	IEC (mmol/g membrane)	IEC (mmol/g Nafion[®])
	1	0.2162	6.2000	0.1550	0.7169	0.7878
	2	0.1641	4.8000	0.1200	0.7313	0.8035
	3	0.2243	6.7000	0.1675	0.7468	0.8206
	Mean				0.7317	0.8040
	S.D.				0.0149	0.0111

ศูนย์วิทยทรัพยากร
จุฬาลงกรณ์มหาวิทยาลัย

Appendix D

Mechanical Properties

Table D-1 Tensile Properties of Pristine Nafion[®] Membrane under Room Condition

specimens	minimum thickness (mm)	minimum cross sectional area (mm^2)	maximum load (N)	load at yield point (N)	initial slope E-modulus (MPa)	elongation at break (%)
1	0.300	3.00	53.53	8.24	214.00	327.00
2	0.267	2.67	32.80	4.40	150.00	264.00
3	0.238	2.38	28.78	4.45	175.00	271.00
4	0.167	1.67	31.64	7.08	237.50	264.00
5	0.193	1.93	28.95	5.34	214.29	261.00
A.V.					198.16	277.40
S.D.					35.05	27.97

Table D-2 Tensile Properties of Pristine Nafion® Membrane under Hydrated Condition

specimens	minimum thickness (mm)	minimum cross sectional area (mm^2)	maximum load (N)	load at yield point (N)	initial slope E-modulus (MPa)	elongation at break (%)
1	0.314	3.14	37.35	5.59	140.00	146.00
2	0.259	2.59	38.90	4.21	130.00	212.00
3	0.325	3.25	55.38	5.08	121.43	243.00
4	0.347	3.47	43.99	10.07	111.11	118.00
5	0.353	3.53	54.98	9.59	103.57	206.00
A.V.					121.22	185.00
S.D.					14.52	51.34

Table D-3 Tensile Properties of Nafion®/ 3 phr m-MMT Composite Membrane under Hydrated Condition

specimens	minimum thickness (mm)	minimum cross sectional area (mm^2)	maximum load (N)	load at yield point (N)	initial slope E-modulus (MPa)	elongation at break (%)
1	0.330	3.30	20.70	4.84	131.25	21.00
2	0.333	3.33	23.96	5.20	110.00	49.00
3	0.337	3.37	27.45	4.84	133.33	94.00
4	0.320	3.20	25.30	4.67	115.38	94.00
5	0.338	3.38	18.22	4.62	107.14	35.00
A.V.					119.42	58.60
S.D.					12.14	33.80

Table D-4 Tensile Properties of Nafion$^{®}$/ 6 phr m-MMT Composite Membrane under Hydrated Condition

| specimens	minimum thickness (mm)	minimum cross sectional area (mm^2)	maximum load (N)	load at yield point (N)	initial slope E-modulus (MPa)	elongation at break (%)
1	0.327	3.27	28.89	4.43	125.00	123.00
2	0.320	3.20	23.66	6.98	110.00	125.00
3	0.330	3.30	22.84	4.81	100.00	107.00
4	0.327	3.27	26.62	8.51	106.25	145.00
5	0.309	3.09	23.32	6.22	116.67	74.00
A.V.					111.58	114.80
S.D.					9.63	26.50

Table D-5 Tensile Properties of Nafion$^{®}$/ 10 phr m-MMT Composite Membrane under Hydrated Condition

specimens	minimum thickness (mm)	minimum cross sectional area (mm^2)	maximum load (N)	load at yield point (N)	initial slope E-modulus (MPa)	elongation at break (%)
1	0.324	3.24	27.44	5.10	125.00	79.00
2	0.334	3.34	25.95	4.12	130.00	69.00
3	0.330	3.30	23.13	4.28	114.29	65.00
4	0.322	3.22	26.60	4.66	131.25	67.00
5	0.341	3.41	23.98	4.30	114.00	75.00
A.V.					122.91	71.00
S.D.					8.33	5.83

Appendix E

Publication

The Pure and Applied Chemistry International Conference 2009 was taken place on 14 - 16 January 2009 at Naresuan University, Phitsanulok, Thailand. Part of this thesis was published on the "PACCON 2009 Proceedings", in the section of "Material Science and Nanotechnology" on page of 335 - 337 as shown below.
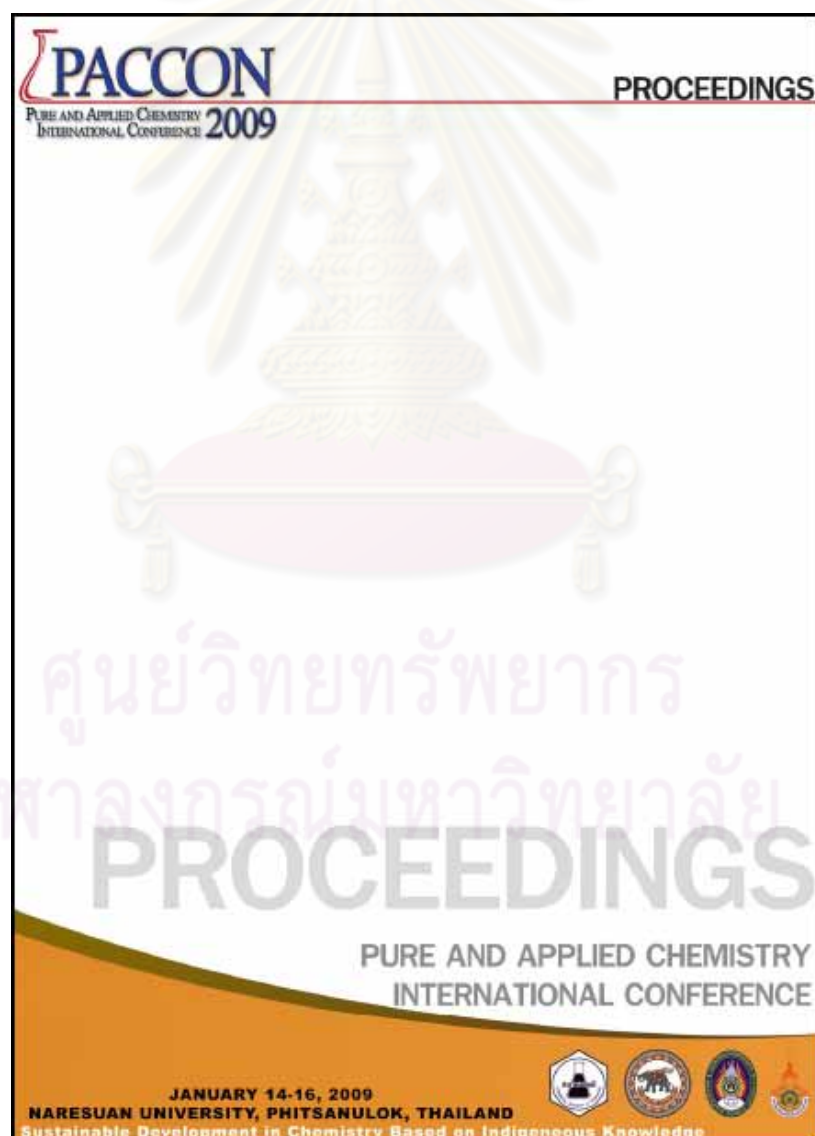
EFFECTS OF MODIFIED ORGANO-CLAY ON THE MECHANICAL PROPERTIES OF FUEL CELL MEMBRANE

Pitch Sakwong[1] and Varun Taepaisitphongse[1*]

[1]Department of Chemical Engineering, Faculty of Engineering, Chulalongkorn University, Bangkok 10330, Thailand

*E-mail: varun.s@chula.ac.th

Abstract: Modified montmorillonite (m-MMT) clay shows an excellent barrier effect for methanol permeability of composite membrane in Direct Methanol Fuel Cell application. However, there are little information about mechanical properties improvement of Nafion®/m-MMT composite membrane. In this paper Nafion®/m-MMT composite membranes were prepared by solution mixing method with m-MMT in the ranges of 0-10 phr. The structure of composite membranes was studied by XRD. The performance of the Nafion®/m-MMT composite membranes were determined in terms of water uptake, ion exchange capacity (IEC), and their mechanical properties. The XRD results showed the m-MMT was not intercalated into Nafion®. Therefore, the mechanical properties of composite membranes were not much improved. However, water uptake and IEC of Nafion®/MMT composite membranes were not significantly changed with increasing m-MMT clay contents.

Introduction

Direct methanol fuel cell (DMFC) is one of the most promising candidates as a power source for electronic devices and transportation applications because DMFC offers high power density, low operating temperature and easy handling of the fuel [1-3]. Perfluorosulfonate ionomer (PFSI), such as Nafion®, is equipped into fuel cell device to provide proton conduction from anode to cathode. Nafion® membrane shows some excellent properties such as chemically inert and high proton conductivity but some disadvantages such as high methanol permeability [1]. Montmorillonite (MMT) clay is a layered structure of aluminum octahedron between two layers of silicon tetrahedron. It has high surface area, negative charge, low thermal expansion and is easy to disperse in water. The barrier properties, mechanical properties and thermal stability of polymers can be improved by incorporating MMT into the polymer matrix [2, 4]. Previous works [1-6] had attempted to reduce the methanol permeability and improve proton conductivity of Nafion® membrane by preparing Nafion®/modified-Montmorillonite (m-MMT) composite membrane. The addition of m-MMT into Nafion® matrix resulted in a decreasing of methanol permeability by approximately 40-50%. However, the proton conductivity of Nafion®/m-MMT composite membrane was lower than that of pristine Nafion® membrane [2, 5, 6]. But, there was little information

about the improvement of mechanical properties of the Nafion®/m-MMT composite membrane.

Nafion®/m-MMT composite membranes were prepared by solution mixing method in this work to study the effects of m-MMT on mechanical properties of composite membrane. The characteristics of the composite membrane were analyzed in terms of mechanical properties, water uptake, ion exchange capacity (IEC) and XRD pattern.

Materials and Methods

Preparation of Composite Membrane: The composite membranes were prepared as follows. A desired amount of m-MMT (Bentone SD®1, supplied by Connell Bros. (Thailand) Co., Ltd.) was added into 5 wt% Nafion® perfluorinated resin solution (purchased from Sigma Aldrich Co., Ltd.), then stirred mechanically for 3 hr and degassed by ultrasonication for 2 hr. The contents of m-MMT at 3, 6 and 10 phr were used. The prepared mixture was then poured into Petri dish and dried in vacuum oven by slowly increasing the temperature from 0 to 85 °C to prevent the crevice in the composite membrane. Finally, the composite membrane was pre-treated in a standard manner: boiled in 5% H_2O_2 solution at 80 °C for 1 hr, boiled in 1 M H_2SO_4 solution at 80 °C for several hours, and boiled in deionized water at 80 °C for 1 hr.

Physical Characterization: Inter-layer spacing between clay platelets of m-MMT in the membranes and the ion channel size of Nafion® matrix were measured by X-ray diffraction (XRD) with Bruker AXS Model D8 Discover with CuKα radiation. The voltage and the current of x-ray beams were 40 kV and 40 mA, respectively. XRD data were collected between 1 and 20° by step of 0.025° with scan speed of 1 second/step.

Ion Exchange Capacity (IEC) Measurement: IEC (mmol of proton per dry weight of membrane) was measured by titration method. The acid form membranes were weighed and then soaked in 1 M NaCl solution for 24 h to fully exchange sodium ions for the protons in the membranes. The exchanged protons were titrated with NaOH solution using phenolphthalein as indicator. The experiments were repeated 3 times and the average IEC was reported. The IEC was calculated by following equation:

$$IEC = \frac{C_{NaOH}V_{NaOH}}{W_{dry}}$$

Where C_{NaOH} and V_{NaOH} are molar concentration and titration volume of NaOH solution, respectively, and W_{dry} is dry weight of membrane.

Water Uptake: The composite membranes were dried in vacuum oven at 100 °C for 24 h and weighed. The membranes were then immersed in deionized water for 24 h and weighed. The water uptake of membranes was calculated using the following equation:

$$Water\, Uptake = \frac{W_{wet} - W_{dry}}{W_{dry}} \times 100\%$$

Where W_{dry} and W_{wet} are weight of membranes in dried and soaked conditions, respectively.

Tensile properties Measurement: According to ASTM D882 for tensile properties of thin plastic sheeting, the composite membranes were cut into the rectangular specimens (1 cm x 10 cm). The prepared test specimens were tested by Instron[®] 5567 instrument with the initial distance between grips of 5 cm and the rate of grips separation of 5 mm/min.

Results and Discussion

XRD analysis: The XRD patterns of pristine Nafion[®] and Nafion[®]/ m-MMT composite membranes with various clay contents were shown in Figure 1. From the Bragg's law ($2d \sin \theta = \lambda$), the ion channel size of Nafion[®] membrane was reduced from 7.99 nm (occurred at $2\theta = 1.10°$ in Fig. 1(a)) to average of 3.06 nm (occurred at approximately $2\theta = 2.72°$ in Figs. 1(c), 1(d), 1(e)) when m-MMT were added. The smaller channel size in composite membrane could lead to the reduced the methanol crossover [3].

However, the d-spacing of interlayer of m-MMT of 1.39 nm in the Nafion[®]/m-MMT composite membrane (occurred at approximately $2\theta = 6.35°$ in Figs. 1(c), 1(d), 1(e)), was smaller than that of m-MMT clay at 3.71 nm (occurred at $2\theta = 2.38°$ in Fig. 1(b)). This suggested that the Nafion[®] matrix did not intercalate into the interlayer spacing of m-MMT. Therefore, these composite membranes were the conventional composite.

IEC and water uptake: Water uptake and IEC are closely related to the proton conductivity and mechanical strength of proton conducting membrane [2]. The values of water uptake and IEC of samples in this work were shown in Table 1. The water uptake of Nafion[®]/m-MMT (10 phr) composite membrane was increased by 36.45% from the pristine Nafion[®]. The increase in water uptake might be due to m-MMTs which were hydrophilic filler. Ion exchange capacities (IECs) of composite membranes were lower than that of pristine Nafion[®]. This may be due to lower amount of Nafion[®] in the composite membrane than the pristine Nafion[®] membrane when compared at equal total weight. This decreasing in IEC was conformed to the previous study [2]. Moreover, it suggested that there were no counter ions located between the interlayer of m-MMT.

The proton conductivity of Nafion[®] membrane depends on the amount of counter ion and water retention in the membrane [3]. Although the IECs of composite membranes prepared here were decreased but the water uptakes were increased. Hence, the overall proton conductivity of composite membranes should not change much from the pristine Nafion[®].

Tensile Properties: Before the tensile properties were tested, Nafion[®]/m-MMT composite membranes were cut into rectangular specimens and then they were soaked in the water for 24 hr. The fully-hydrated
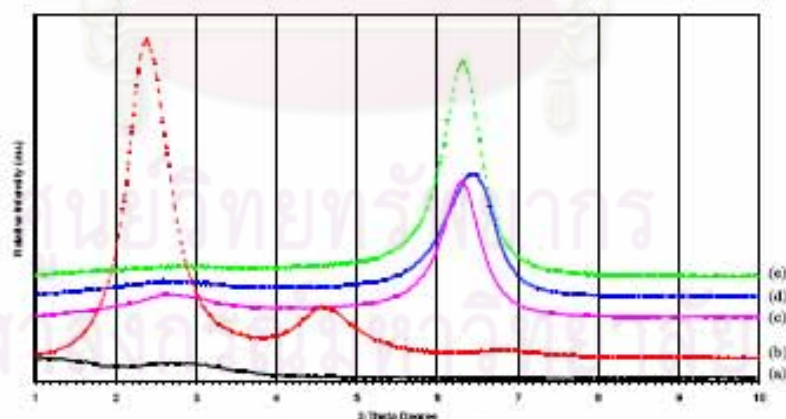

Figure 1. XRD patterns of pristine Nafion[®] (a), m-MMT (b), Nafion[®]/m-MMT composite membrane containing m-MMT at 3 phr (c), 6 phr (d), and 10 phr (e).

Table 1: Water uptake and IEC values of Nafion®/m-MMT composite membranes

Membrane	Water Uptake (%)	IEC (mmol/g)
Pristine Nafion®	20.3	0.89
Nafion®/m-MMT 3 phr	25.6	0.79
Nafion®/m-MMT 6 phr	26.0	0.76
Nafion®/m-MMT 10 phr	27.7	0.73

specimens were tested by Instron® 5567 universal testing machine. The results were shown in Figure 2. The Young's modulus (103 MPa) and elongation at break (206 %) of the composite membrane (at 0 phr m-MMT) prepared in this work were similar to data given for commercially available Nafion® membrane (114 MPa and 200 %, respectively) [8].

Figure 2 showed that elastic modulus of the composite membranes increased with increasing amount of m-MMT. The Young's modulus of composite membrane was increased from 103 MPa to 125 MPa for the contents of m-MMT from 0 to 10 phr. This small increment of elastic modulus may be because the composite membrane was a conventional type.
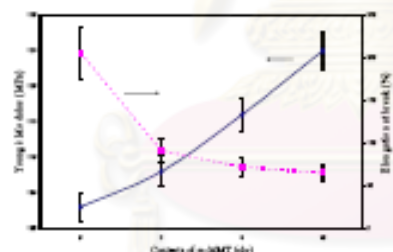

Figure 2. Tensile properties of soaked Nafion®/m-MMT composite membrane with various amount of m-MMT.

The elongation at break of the composite membranes decreased with increasing amount of m-MMT. The elongation at break of composite membrane was decreased from 206 % to 65 % for the contents of m-MMT from 0 to 10 phr. The result was somewhat expected as polymer incorporated with filler normally is harder but more brittle than the neat polymer.

Conclusion

The effect of incorporation of m-MMT into Nafion® matrix to form composite membrane by solution mixing method was studied. The XRD patterns showed that the interlayer spacing of m-MMT was decreased when incorporated into Nafion® matrix and the Nafion® did not intercalate into interlayer of m-MMT. Hence, the Nafion®/m-MMT composite membrane was in case of conventional composite. Therefore, the mechanical properties were not much improved. However, the water uptakes of composite membranes were slightly increased and the IECs were decreased with increasing amount of the filler. Therefore, the proton conductivity of Nafion®/m-MMT composite membranes should not be much different from the pristine Nafion® membrane.

References:

[1] F. Mura, R.F. Silva, A. Pozio, Electrochimica Acta 52 (2007), pp. 5824-5828.
[2] Y.F. Lin, C.Y. Yen, C.C.M. Ma, S.H. Liao, C.H. Hung, Y.H. Hsiao, Journal of Power Sources 165 (2007), pp. 692-700.
[3] C.H. Rhee, Y. Kim, J.S. Lee, H.K. Kim, H. Chang, Journal of Power Sources 159 (2006), pp. 1015-1024.
[4] L. Zhang, J. Xu, G. Hou, H. Tang, F. Deng, Journal of Colloid and Interface Science 311 (2007), pp. 38-44.
[5] Y. Kim, J.S. Lee, C.H. Rhee, H.K. Kim, H. Chang, Journal of Power Sources 162 (2006), pp. 180-185.
[6] J.-M. Thomassin, C. Pagnoulle, G. Calderella, A. Germain, R. Jerome, Polymer 46 (2005), pp.11389-11395.
[7] J. Pan, H. Zhang, M. Pan, Journal of Colloid and Interface Science 326 (2008), pp. 55-60.
[8] http://www.fuelcells.dupont.com

VITA

Mr.Pitch Sakwong was born in Lampang, Thailand on January 2, 1985. He completed high school at Boonyawat Wittayalai School, Lampang, Thailand in 2002 and received a Bachelor degree of Chemical Engineering from the Department of Chemical Engineering, Faculty of Engineering, Kasetsart University, Bangkok, Thailand in 2006. He began study for Master of Engineering degree at the Department of Chemical Engineering, Faculty of Engineering, Chulalongkorn University, Bangkok, Thailand in 2006.